CZECH TECHNICAL UNIVERSITY IN PRAGUE
Faculty of Electrical Engineering
Department of Telecommunication Engineering

Four Wave Mixing in Optical Networks using DWDM

Master's thesis

Bc. Anastasiya Shkalikava
Supervisor: Ing. Michal Lucki, Ph.D.

Prague, May 2018

Čestné prohlášení

Prohlašuji, že jsem zadanou diplomovou práci zpracoval sám s přispěním vedoucího práce a konzultanta a používal jsem pouze literaturu v práci uvedenou. Dále prohlašuji, že nemám námitek proti půjčování nebo zveřejňování mé diplomové práce nebo její části se souhlasem katedry.

Datum: 25. 5. 2018

.....

Bc. Anastasiya Shkalikava

Poděkování

Mé poděkování patří panu Ing. Michalu Luckimu, PhD. za odborné vedení, za pomoc, vstřícnost při konzultacích a cenné rady při zpracování této práce. Děkuji také za pomoc při gramatické kontrole práce.

ZADÁNÍ DIPLOMOVÉ PRÁCE

I. OSOBNÍ A STUDIJNÍ ÚDAJE

Příjmení: **Shkalikava** Jméno: **Anastasiya** Osobní číslo: **411209**

Fakulta/ústav: **Fakulta elektrotechnická**

Zadávající katedra/ústav: **Katedra telekomunikační techniky**

Studijní program: **Elektronika a komunikace**

Studijní obor: **Komunikační systémy a sítě**

II. ÚDAJE K DIPLOMOVÉ PRÁCI

Název diplomové práce:

Čtyřvlnné směšování u optických sítí s hustým vlnovým multiplexem

Název diplomové práce anglicky:

Four Wave Mixing in Optical Networks using DWDM

Pokyny pro vypracování:

Cílem práce je experiment a simulace jevu čtyřvlnného směšování (FWM) v optických sítích. Dílčím cílem je prozkoumání vlivu jevu čtyřvlnného směšování na vybrané optické sítě používající hustý vlnový multiplex a optoelektronické zesilovače. Dalším cílem je prozkoumání kombinace jevu FWM s jinými nepříznivými faktory, např. disperzi, PMD, nedodržením kanálové rozteče nebo výkonových úrovní. Simulace provádějte v prostředí Optsim a s ohledem na doporučení ITU-T v této oblasti. Dalším cílem je experiment - vybuzení FWM na cívce s vláknem s téměř nulovou disperzí, s použitím dostupných laserů, vláken a spektrálního analyzátoru a porovnání experimentálních výsledků se simulacemi.

Seznam doporučené literatury:

[1] Agrawal, G.P.: Lightwave Technology: Telecommunication Systems, Wiley Interscience, USA, New Jersey, 2005. ISBN: 978-0-471-21572-1.
[2] Freude, W.; Schmogrow, R.: Quality Metrics for Optical Signals: Eye Diagram, Q-factor, OSNR, EVM and BER, in Proceedings of 14th International Conference on Transparent Optical Networks, Coventry, England, paper Mo.B1.5, 2012.
[3] ITU-T G-series Supplement 39: Transmission systems and media, digital systems and networks. ITU, 2012. Dostupné na http://www.itu.int/rec/T-REC/en [on-line]

Jméno a pracoviště vedoucí(ho) diplomové práce:

Ing. Michal Lucki, Ph.D., katedra telekomunikační techniky FEL

Jméno a pracoviště druhé(ho) vedoucí(ho) nebo konzultanta(ky) diplomové práce:

Datum zadání diplomové práce: **04.01.2018** Termín odevzdání diplomové práce: **25.05.2018**

Platnost zadání diplomové práce: **30.09.2019**

Ing. Michal Lucki, Ph.D. podpis vedoucí(ho) práce	podpis vedoucí(ho) ústavu/katedry	prof. Ing. Pavel Ripka, CSc. podpis děkana(ky)

III. PŘEVZETÍ ZADÁNÍ

Diplomantka bere na vědomí, že je povinna vypracovat diplomovou práci samostatně, bez cizí pomoci, s výjimkou poskytnutých konzultací. Seznam použité literatury, jiných pramenů a jmen konzultantů je třeba uvést v diplomové práci.

.	
Datum převzetí zadání	Podpis studentky

© ČVUT v Praze, Design: ČVUT v Praze, VIC

MASTER'S THESIS ASSIGNMENT

I. Personal and study details

Student's name: **Shkalikava Anastasiya** Personal ID number: **411209**

Faculty / Institute: **Faculty of Electrical Engineering**

Department / Institute: **Department of Telecommunications Engineering**

Study program: **Electronics and Communications**

Branch of study: **Communication Systems and Networks**

II. Master's thesis details

Master's thesis title in English:

Four Wave Mixing in Optical Networks using DWDM

Master's thesis title in Czech:

Čtyřvlnné směšování u optických sítí s hustým vlnovým multiplexem

Guidelines:

The goal of the thesis is an experiment and simulations of Four Wave Mixing (FWM) in optical networks. The partial goal is to investigate the FWM effect in selected optical networks using dense wave multiplex and optoelectronic amplifiers. Another objective is to examine the combination of FWM with other unfavorable factors, such as dispersion, PMD, wrong channel spacing or too high power levels. Perform simulations using Optsim environment and with regard to current ITU-T recommendations in this area. Another goal is to run the experiment for FWM using a near-zero dispersion fibers, available lasers, and a spectral analyzer, and to compare the results with the simulations.

Bibliography / sources:

[1] Agrawal, G.P.: Lightwave Technology: Telecommunication Systems, Wiley Interscience, USA, New Jersey, 2005. ISBN: 978-0-471-21572-1.
[2] Freude, W.; Schmogrow, R.: Quality Metrics for Optical Signals: Eye Diagram, Q-factor, OSNR, EVM and BER, in Proceedings of 14th International Conference on Transparent Optical Networks, Coventry, England, paper Mo.B1.5, 2012.
[3] ITU-T G-series Supplement 39: Transmission systems and media, digital systems and networks. ITU, 2012. Dostupné na http://www.itu.int/rec/T-REC/en [on-line]

Name and workplace of master's thesis supervisor:

Ing. Michal Lucki, Ph.D., Department of Telecommunications Engineering, FEE

Name and workplace of second master's thesis supervisor or consultant:

Date of master's thesis assignment: **04.01.2018** Deadline for master's thesis submission: **25.05.2018**

Assignment valid until: **30.09.2019**

Ing. Michal Lucki, Ph.D. Supervisor's signature	Head of department's signature	prof. Ing. Pavel Ripka, CSc. Dean's signature

III. Assignment receipt

The student acknowledges that the master's thesis is an individual work. The student must produce her thesis without the assistance of others, with the exception of provided consultations. Within the master's thesis, the author must state the names of consultants and include a list of references.

Date of assignment receipt	Student's signature

© ČVUT v Praze, Design: ČVUT v Praze, VIC

Anotace

Tato diplomová práce se zabývá zkoumáním vlivu nelineárního jevu čtyřvlnného směšování na optické sítě používající hustý vlnový multiplex (DWDM) a optoelektronické zesilovače. V práci je představeno několik simulací čtyřvlnného směšování v závislosti na různých parametrech a jejich kombinacích, provedených v prostředí Optsim s ohledem na doporučení ITU-T v této oblasti. Dále je v práci také popsáno několik experimentů v laboratorních podmínkách za účelem vybuzení FWM jevu, včetně jeho degenerované varianty. Na konci práce jsou experimentální výsledky porovnány se simulacemi.

Klíčová slova

Čtyřvlnné směšování, Optické sítě, Nelineární jevy v optických sítích, Optický multiplex, DWDM systémy, DWDM rastr, NZDSF vlákno, Optické zesilovače, Optické laserové zdroje, OptSim, Chromatická disperze, Chybovost BER.

Summary

This master's thesis deals with the study of influence of a non-linear phenomenon known as Four Wave Mixing (FWM) on optical DWDM networks using optoelectronic amplifiers. Several simulations of raising FWM depending on different parameters and their combinations are performed in this work. The simulations were carried out in the Optsim environment, taking into account ITU-T recommendations in this area. Several experiments under laboratory conditions were made with the aim to raise FWM, including exemplification of its degenerate form. Experimental results are compared to simulations in order to conceptualize the FWM models and to assess eligibility of the method.

Index Terms

Four wave mixing, Optical networks, Non-linear optical effects, Optical multiplex, DWDM systems, DWDM grid, Optical fibers, NZDSF & DSF, Optical amplifiers, Optical laser sources, OptSim, Chromatic dipersion, Bit Error Rate.

List of Figures

List of Tables

Contents

1 Introduction

Optical communication systems, and especially those with dense channel spacings, are currently essential to telecommunication networks for high bit rate signal transmission to distant places. It is presently the most widely used medium in telecommunications, and therefore study of the problems associated with it is obligatory before any and all improvements in this field.

The main factor affecting the output signal quality, specific to DWDM systems is FWM. It may not be a totally unknown effect, in professional literature there are enough ways to resist it, but technology does not stay in one place - someday soon a new DWDM-like implementation may be created, that would be very vulnerable to FWM.

1.1 Problem statement

The primary goal of this work is the study of four wave mixing phenomenon, including its degenerate form in a DWDM based network using simulation environment OptSim or under laboratory conditions. When FWM is obtained, the partial goal is to investigate the influence of said FWM on the composed network using optoelectronic amplifiers. The next goal is to examine combinations of FWM phenomenon with other adverse factors, such as dispersion, and not keeping the recommended channel spacing or power levels. Practical experiments were made using a 50-km long spool of fiber with near-zero dispersion, and some commonly available telecommunication lasers and fibers, and a spectrum analyzer. All the results obtained via experiments and simulations are to be analyzed and compared.

1.2 Thesis arrangement

The introductory part of this work is focused on non-linear effects in optical networks, and concentrates primarily at FWM, where, as well, are described the ways of FWM compensation while in optical transmission.

The sixth chapter demonstrates the results of simulations made in the OptSim environment, where different parameters and their combinations are tested. The TDSS method for calculating the optical signal propagation is employed in OptSim and the ways of simulation result monitoring are described in the fifth chapter.

Practical experiment is reported in the eighth chapter, where the influence of FWM on the output signal is analysed in relation with varied parameters. The experiment is performed for Degenerate and Non-Degenerate FWM types. This chapter also shows the comparison of the simulation and experimental results.

The work's conclusion includes the evaluation of conditions that lead to FWM generation in optical networks, as well as recommendation on how to avoid or minimize its adverse effects.

2 Types of non-linear effects in DWDM

> *"Optical light wave is not only driven by a fiber but also have influence on the fiber, and each signal inside it changes the conditions of transferring of the other signals in a certain way."* prof. Ing. Jan Sýkora, CSc.

In Dense Wavelength Division Multiplexing system (DWDM), which offers component reliability, system availability and system margin, the nonlinear effects play important role. They can greatly affect the transmission properties and the spectral efficiency of DWDM optical system. With increasing power level carried by fiber are generated nonlinear effect such as SPM, XPM, SRS, SBS and FWM.

- Self-phase modulation (SPM). This effect appears due to dependence of refractive index on light intensity: in those parts of pulse where the intensity is going higher, the refractive index is increasing, along with the wavelength. Following the previous definition, the immediate carrier frequency is decreasing with ascending part of pulse (shift to IR frequencies), and on the contrary, the immediate carrier frequency is increasing in descending part of pulse (shift to UV). This frequency change in combination with chromatic dispersion (CD) leads to the change of pulse shape over time. The temporary frequency change is known as "chirp". [26]

- Cross-phase modulation (XPM). It is a special case of SPM, where the refractive index is not only affected by the pulse itself, but also by other pulses transmitted by the fiber at the same time on different wavelengths. The same as SPM, XPM leads to a change in the frequency spectrum, that in combination with the CD leads to a change in pulse shape over time.

- Stimulated Raman Scattering (SRS) and Stimulated Brillouin Scattering (SBS). Both phenomena describe nonlinear light scattering where new light of a different frequency is generated. Newly generated photons are referred to Stokes particles, if part of energy is lost and their frequency is lower, than the original light. In case that the new photons were supplied with a part of energy and thus their frequency is higher, they are called Anti-Stokes particles. In both of these variations, the generation and performance of the scattered light increases strongly when a certain threshold level is exceeded. In general, the broader the spectrum of the optical source signal, the higher the threshold power.

  In case of Stimulated Brillouin Scattering, which is spreading backward, a powerful light wave travels through a fiber and interacts with acoustical vibration modes in the glass. The newly generated light wavelength differs only in the order of several GHz from the

original one, and the bandwidth in which the light is located is only units of tens of MHz. The Brillouin scattering power threshold for classical SM fibers is in the order of tens of mW and is strongly dependent on the fiber composition, the width of the source spectrum, the transfer rate, and the modulation used.

Raman's scattering, unlike Brillouin's scattering, is omni-directional. When the threshold is exceeded, some of the scattered light is scattered in the same direction as the working optical signal, but a portion of the scattered energy is exported out of the fiber outward and a portion advancing back to the beginning of the fiber. Moreover, it leads to changes in its wavelength, which can be qualified as a loss of energy at the working wavelength. Therefore, Raman scattering may cause problems with the broadband DWDM system, where the optical power from higher frequency channels is transfered to lower frequency channels (Stokes). on the other hand, this effect can be used to intensify all channels through the SRS phenomenon. This is why Raman's phenomenon is being used to construct an optical amplifier. [14]

- Four-Wave Mixing (FWM). FWM occurs when two or more waves of near frequencies are launched into a fiber, giving rise to a new wave of different wavelength, known as an idler. It is the most significant non-linear effect because of the largest influence on transfered signal, this is why this work is dedicated to studying the FWM effect and investigating of interaction of its properties and signal propagation medium.

3 Four-Wave Mixing (FWM)

FWM is one of the major limiting factors in DWDM optical communication systems that use narrow channel spacing and low or almost zero dispersion fibers.

If two or more channels in a fiber interact with one another through FWM, it causes additional noise on the system and degrades the signal quality. The newly generated frequencies appear at the cost of reduction of power at the original optical wavelengths. Power is lost from desired signals due to unwanted ones. When this fourth wavelength acts as an interfering signal to the original one, the retrieval of the original signal is difficult. This is why it is very important to take steps to prevent from FWM or suppress FWM effect in multichannel optical communication systems. Detailed analysis how to avoid FWM is described in section 3.2.

3.1 Theory

This phenomenon occurs in DWDM system because of non-linear susceptibility in optical fiber when three wavelengths of near frequencies propagate together giving rise to the new fourth wavelength. For three continuous-wave channels of input powers P_i, P_j, P_k at frequencies f_i, f_j, f_k the intermodulation products will appear at frequencies [19]:

$$f_4 = \pm f_i \pm f_j \pm f_k. \tag{1}$$

We do not pay attention to all the frequency combinations of equation 1, for example $f_i + f_j + f_k$, because these frequencies lay out of the telecommunication band that is of particular importance since such waves may easily be eliminated by filtering process. The amount of intermodulation products which are really important from the point of view of encumbering noise is [19]:

$$M = \frac{1}{2} \cdot N^2 \cdot (N - 1). \tag{2}$$

The number of generated FWM products grows exponentially with number of channels, as demonstrated on graph 1. For example, optical systems with 40 channels have around 30000 FWM products while for such systems with 80 channels this number reaches over 250000.

New frequencies laying inside the readable band and generated by three continuous wave channels are:

$$
\begin{aligned}
f_i + f_j - f_k,\\
f_i + f_k - f_j,\\
f_j + f_k - f_i,\\
2f_i - f_j, 2f_i - f_k,\\
2f_j - f_i, 2f_j - f_k,\\
2f_k - f_i, 2f_k - f_j.
\end{aligned}
\tag{3}
$$

You can have a more detailed look in section 8.2, where precious FWM wavelength were calculated and compared with real arose FWM products from the mensuration on the required spectrum band.

Then the power of the light-wave resulting from FWM at the frequency is [13]:

$$P_{ijk} = d_{ijk}^2 \gamma^2 L_{eff}^2 P_i P_j P_k \eta_{ijk} e^{-\alpha z}, \tag{4}$$

where d_{ijk} is the degeneracy factor, which takes value 1 and 2 for degenerate ($i = j$) and non-degenerate ($i \neq j$) terms respectively, L_{eff} is the effective length, η_{ijk} is FWM efficiency, α is an optical attenuation in dB/km, z is the length of fiber in km, γ is the nonlinear coefficient, which is given by equation [13]:

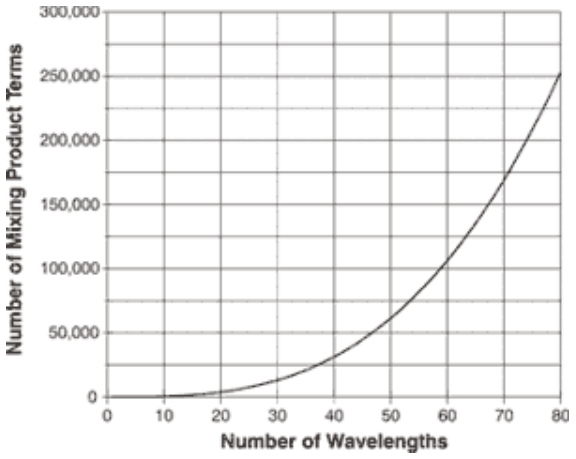

Figure 1: Number of FWM products depending on number of channels [2]

$$\gamma = \frac{(2\pi n_2)^2}{A_{eff}^2} \cdot \frac{1}{\lambda^2}, \tag{5}$$

where n_2 is the fiber nonlinearity coefficient, A_{eff} is the core effective cross-sectional area, λ is the central wavelength. [31]

3.2 Methods to avoid FWM product creation

- **Using of Non-Zero Dispersion Shifted Fibers (NZDSF)**

  It is a generally accepted view that chromatic dispersion causes pulse spreading in time, which is a substantial problem for pulses travelling over long distances. Because of that reason do exist optical fibers which compensate for dispersion.

  What we just call dispersion is a sum of two factors: material dispesion, which is determined by material of the fiber and therefore is non-adjustable, and waveguide dispersion, which can be modified by changing of refractive index profiles in fibers. This

waveguide dispersion is used to compensate material dispersion. Characteristics of a single-mode optical fibre cable specified at ITU-T G.652 [24] have zero dispersion at wavelength $\lambda = 1310$ nm. Some time after this specification long-distance telecommunication networks began to mainly use wavelengths around $\lambda = 1550$ nm, which led to the developement of Dispersion Shifted Fibers (DSF) specified at ITU-T G.653 [22]. Such fibers have zero dispersion at wavelength $\lambda = 1550$ nm. DWDM systems though are incompatible with such fibers because multiple channels and zero chromatic dispersion add up to the creating of serious FWM crosstalks. Having said problem in mind, Non-Zero Dispersion Shifted Fibers (NZDSF) were specified in ITU-T G.655 [21] in order to let DWDM achieve its maximum efficiency by setting low, but non-zero dispersion value at 1550 nm, so that signal could travel long distances without causing crosstalks.

- **Spacing channels unequelly**

  It is a more damaging variant, when FWM generates new wavelengths at frequencies that coincide with channels that carry a useful signal. In this case FWM noise interferes the most. An investigation was conducted in section 8.2 about the influence of channel spacing on FWM product spectral position.

- **Use of the dual-phase amplifier model**

  Usually high power of amplifiers cause FWM effect in DWDM systems. To avoid FWM, instead of one amplifier or a cascade of amplifiers one by one, the first amplifier should be inserted before the optical fiber and the other one behind the fiber. The power of these amplifiers should not be high. Such model is called dual-phase amplifier, which does not cause FWM effect, and power at the output of the cascade is not reduced. The efficiency of this model is verified in section 8.5.

- **Using the correct channel spacing**

  DWDM has a channel spacing less than 1 nm. According to the ITU-T G.694.1 recommendation, describing safe usage of channel frequencies over the total frequency band, the channel spacing can be set as follows:

  - channel spacing 100 GHz (0.8 nm),
  - channel spacing 50 GHz (0.4 nm),
  - channel spacing 25 GHz (0.2 nm),
  - channel spacing 12.5 GHz (0.1 nm).

  About 40 channels with 100 GHz spacing can occupy the complete C-band of 1530-1565 nm. Of course, the number of channels can double when using a channel spacing of 50 GHz.

  Recommended channel spacing is described in more detail in section 4. The use of specific frequencies is given in table 11 by ITU-T.

4 Nominal Central Frequencies of the DWDM Grid

Since DWDM (Dense Wavelength Division Multiplexing) technology is characterized by narrower channel spacing than Coarse WDM, DWDM transmitters require specific demands so that the output signal could be easily deciphered. For this purpose ITU-T comes with recommendation G.694.1 describing safe usage of channel frequencies over the total frequency band. Recommendation G.694.1 supports a variety of fixed channel spacings ranging from 12.5 GHz to 100 GHz and wider (integer multiples of 100 GHz) as well as a flexible grid. [23]

4.1 Fixed DWDM grid frequencies

The channel spacing steps for the fixed grid are determined by sub-division of the initial 100 GHz grid by factors of two. The allowed channel frequencies (in THz) are defined by:

- $193.1 + n \cdot 0.0125$ for channel spacings of 12.5 GHz, where n is a positive or negative integer including 0
- $193.1 + n \cdot 0.025$ for channel spacings of 25 GHz, where n is a positive or negative integer including 0
- $193.1 + n \cdot 0.05$ for channel spacings of 50 GHz, where n is a positive or negative integer including 0
- $193.1 + n \cdot 0.1$ for channel spacings of 100 GHz, where n is a positive or negative integer including 0

Table 11 illustrates some nominal central frequencies within the C and L bands on the 12.5 GHz, 25 GHz, 50 GHz and 100 GHz channel spacing. Conversion between frequency and wavelength is performed using the value of speed of light in vacuum $c = 2.99792458 \cdot 10^8 m/s$.

4.2 Flexible DWDM grid

For the flexible DWDM grid, the allowed frequency slots have a nominal central frequency (in THz) defined by:

- $193.1 + n \cdot 0.00625$, where n is a positive or negative integer including 0, which means that each slot must be able to be divided by 6.25 so that it could be shifted by $n \cdot 0.00625$ THz towards the initial 193.1 THz central frequency,
- and a slot width defined by: $12.5 \cdot m$, where m is a positive integer and 12.5 is the slot width granularity in GHz.

Flexible spacing DWDM grid was mostly defined to allocate frequency slots with different widths for the sake of optimization for specific channel requirements, e.g. to allow a mixed bit rate or mixed modulation format. Figure 2 shows the example where slots of different widths are placed onto the same frequency band. Two 50 GHz slots and two 75 GHz slots are divided by a guard band between 193.125 THz and 193.18125 THz. In this case the slot between 193.18125 THz and 193.25625 THz has parameters $n = 19$, which means that the central frequency was shifted by $19 \cdot 0.00625$ ($193.21875 - 193.1 = 19 \cdot 0.00625 = 0.11875$) THz towards the nominal central frequency 193.1 THz and parameter $m = 6$, which "tells" that the slot consists of $6 \cdot 12.5$ GHz parts. The guard band could also be filled in by other slots, for example by additional slot with a width of 50 GHz ($n = 8, m = 4$), leaving 6.25 GHz unallocated, or a 25 GHz ($n = 6, m = 2$) slot and two 12.5 ($n = 9, m = 1$ and $n = 11, m = 1$) GHz slots, etc.

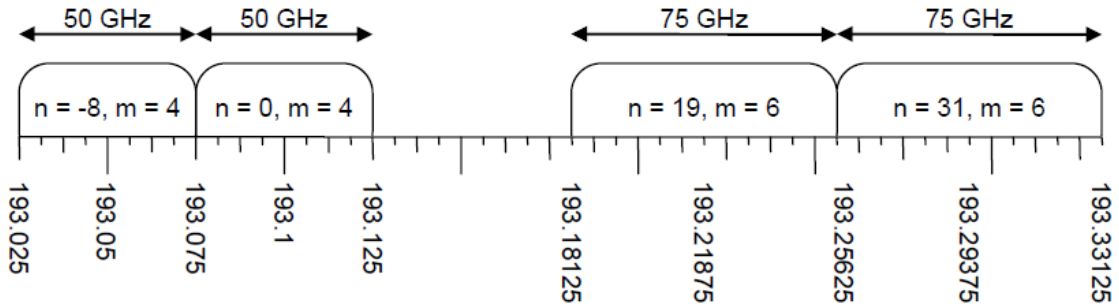

Figure 2: Example of utilizing the flexible DWDM grid with the purpose of using different slot widths [23]

Flexible spacing DWDM grid may be also used with the aim to achieve better transmission parameters due to limited technological capabilities of the system. Figure 3 shows the application of this case.

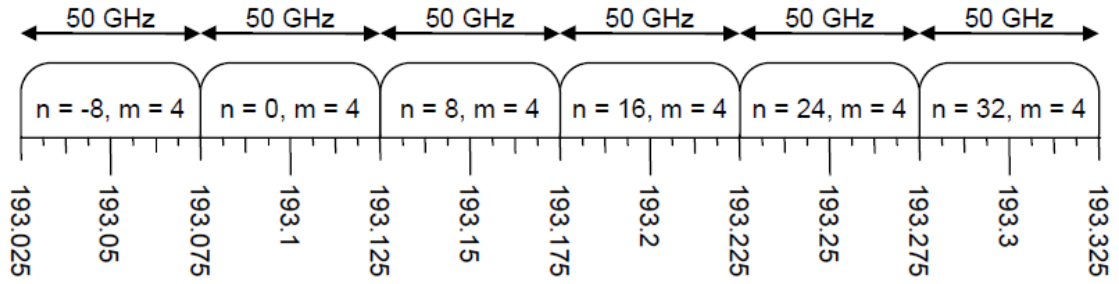

Figure 3: Example of utilizing the flexible DWDM grid with the purpose of avoiding imperfect transmission parameters due to limited technological capabilities of the system [23]

Figure 7 represents the way how slots of custom widths can be relocated so as to avoid the gap between neighboring slots. The condition of slot bandwidths and shift lengths still stands.

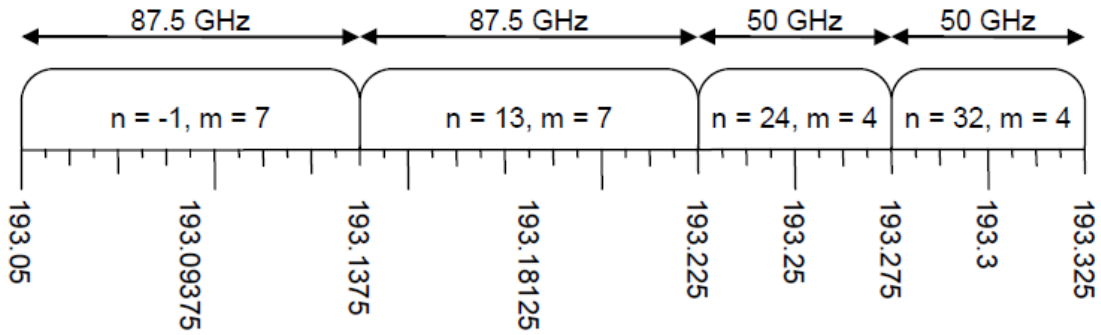

Figure 4: Example of utilizing the flexible DWDM grid with the purpose of using non-standard slot widths [23]

5 OptSim environment

All the simulations introduced in this work were performed by using the OptSim environment. RSoft OptSim provides time-domain split-step (TDSS) engine, which allows to realize the signal distribution equation in a fiber.

5.1 TDSS method

In order to calculate optical signal propagation the following equation is employed in TDSS [8]:

$$\frac{\partial A(t,z)}{\partial t} = \{L + N\} \cdot A(t,z), \tag{6}$$

where $A(t,z)$ is the optical field intensity, L is the operator related to dispersion and other linear effects, N is the operator responsible for all nonlinear effects. This algorithm calculates $A(t,z)$ each fiber span ∂z applying L and N operators. TDSS uses the convolution product in the discrete time [8]:

$$A_L[n] = A[n] * h[n] = \sum_{k=-\infty}^{+\infty} A[k] * h[n-k], \tag{7}$$

where $h[n]$ is the impulse response of L.

Essentially, two ways of calculation are possible: TDSS described above and FDSS (frequency-domain split-step). The second one calculates linear L operator in a frequency domain, whereas TDSS – in the time domain, by calculating the convolution product in sampled time. FDSS is a definitely faster method but there may occur errors while calculating, this is why a complex one but more reliable method TDSS is used [12].

5.2 Monitors

The eye diagram is a useful tool for qualitative signal analysis, which provides a view of the evaluation of the transmission system characteristics and allows to diagnose channel errors. It relates to terms such as Optical Signal to Noise Ratio (OSNR), Q-factor and Bit Error Rate (BER). Unlike these parameters, eye diagram lets us find the specific problem that brings additional noise to the system. For example, it is easy to determine such signal distortions as ASE (Amplified Spontaneous Emission) noise, which induces stronger signal level fluctuations in marks than in spaces, or chromatic dispersion resulting in variations of the signal levels, or interaction between linear and nonlinear effects resulting in fluctuations of the signal power at the rising and trailing edges of the signal [20].

1. Eye diagram

   The more the eye is open, the less degraded the system is. The place of the largest eye opening is considered to be the moment of signal sampling. The eye diagram can be also described by the Q-factor parameter.

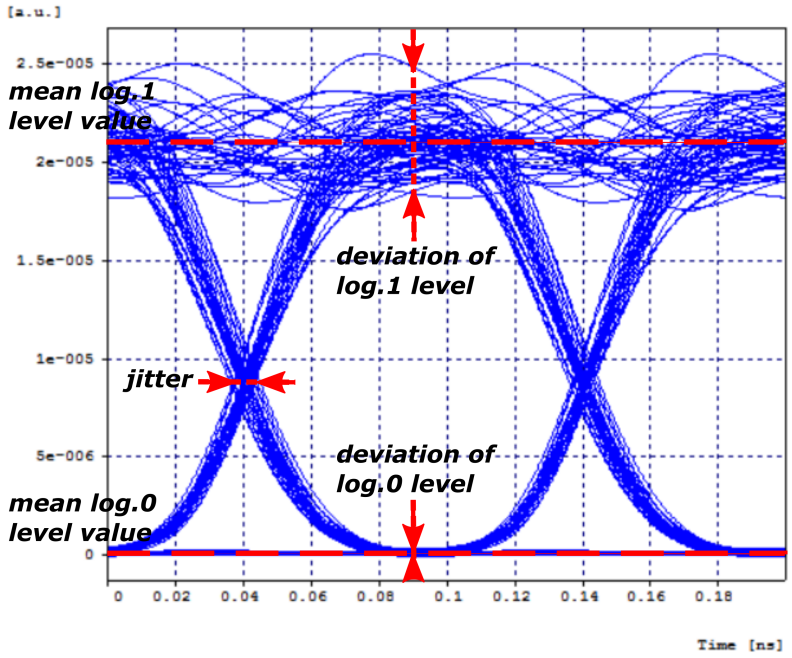

Figure 5: The eye diagram description

2. OSNR and Q-factor

   The OSNR parameter represents the ratio of the optical power of the signal P_s to the noise level P_n in mW [17]:

$$OSNR = 10\log(\frac{P_s}{P_n}). \tag{8}$$

   The Q-factor expresses eye quality. It indicates the effect of interference at the measurement place and means the minimum decision level. It can be calculated as [17]:

$$Q = \frac{\mid \mu_1 - \mu_0 \mid}{\sigma_1 + \sigma_0}, \tag{9}$$

   where μ_0, μ_1 stands for mean log.0, log.1 level values respectively, and σ_0, σ_1 are the corresponding standard deviations, as shown in figure 5.

   Only Q-Factor but not OSNR will be monitored futher in this work because FWM is not measurable in the optical domain.

3. BER

   BER is given by the ratio of received error bits to the total number of received bits. BER and Q-factor are in an inverse relationship: the BER decreases as the Q-factor

increases. The mathematical relation between Q-factor and BER can be expressed as [17]:

$$BER[-] = \frac{1}{2} erfc(\frac{Q}{\sqrt{2}}). \tag{10}$$

Acceptable BER of optical systems which transmission capacity is up to 10 Gbit/s is minimum $BER = 10^{-12}$ [-], but systems over 100 Gbit/s demand at least $BER = 10^{-14}$ [-].

6 Simulation experiments

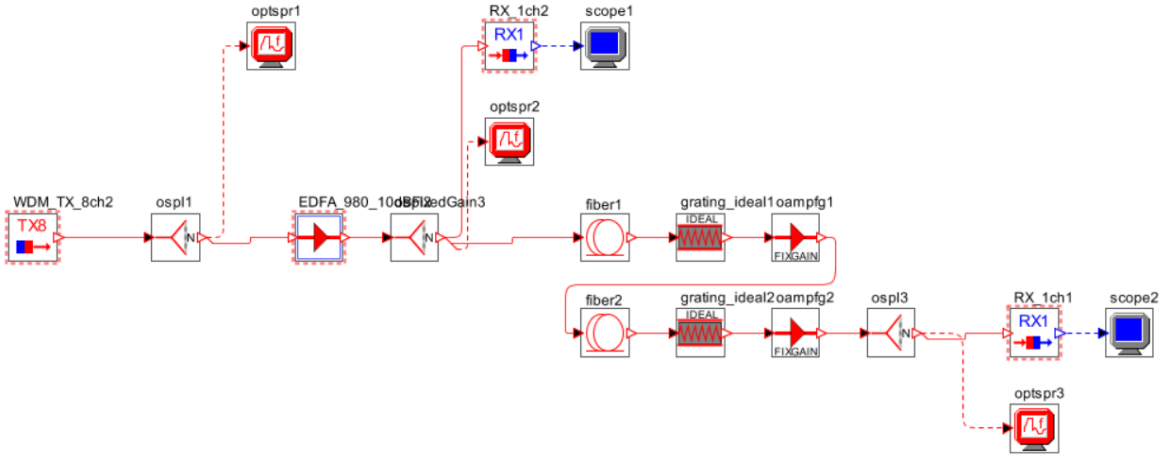

Figure 6: Schematic for testing influence of power of input signal, signal dispersion in fiber and combination of these effects on FWM and BER of output signal. Channel spacing is even – 100 GHz everywhere, spectrum is 192.8 THz – 193.5 THz

6.1 Output signal depending on signal dispersion in fiber

In this chapter the dependence of parameters BER and Q of the output signal on dispersion changes was investigated. The dispersion was changed from 0 to 1 ps/nm/km with step of 0.1 ps/nm/km and then from 1 to 10 ps/nm/km with the step of 1 ps/nm/km. Thus, 20 values were included in table 1. The table is followed by graph 7 representing BER[-] and Q[dB] values depending on fiber dispesion. Pictures of spectral characteristics of output signal, where FWM tops could be observed, and eye diagram of output signal for certain dispersion are located after graph 7.

Dispersion [ps/nm/km]	BER [-]	Q[-]	Q[dB]
0	$2.87 \cdot 10^{-4}$	3.574	11.065
0.1	$6.69 \cdot 10^{-4}$	3.433	10.713
0.2	$2.33 \cdot 10^{-11}$	6.675	16.489
0.3	$6.27 \cdot 10^{-24}$	10.111	20.095
0.4	$1.00 \cdot 10^{-40}$	13.826	22.814
0.5	$1.00 \cdot 10^{-40}$	14.751	23.376
0.6	$5.64 \cdot 10^{-38}$	13.036	22.303
0.7	$1.00 \cdot 10^{-40}$	15.695	23.915
0.8	$1.00 \cdot 10^{-40}$	15.702	23.919
0.9	$1.00 \cdot 10^{-40}$	17.326	24.774
1	$2.40 \cdot 10^{-36}$	12.569	21.986
2	$4.23 \cdot 10^{-23}$	10.004	20.004
3	$6.21 \cdot 10^{-13}$	7.229	17.182
4	$1.23 \cdot 10^{-14}$	7.739	17.774
5	$1.92 \cdot 10^{-14}$	7.673	17.699
6	$6.19 \cdot 10^{-12}$	6.910	16.789
7	$1.07 \cdot 10^{-8}$	5.641	15.027
8	$9.04 \cdot 10^{-6}$	4.291	12.650
9	$4.99 \cdot 10^{-4}$	3.308	10.392
10	$2.66 \cdot 10^{-3}$	2.786	8.901

Table 1: Output signal parameters depending on set signal dispersion in fiber

The first thing that needs to be said is that BER and accordingly Q are decreasing as dispersion increases. It is mostly noticable at values 2 ps/nm/km and higher, where BER at a value of 2 ps/nm/km increases by orderly 10^{-13}, and Q decreases by 2.5, which is 20%. Reliability of optical systems reaches min. BER = 10^{-12}, therefore such an optical network may be used only till D = 6 ps/nm/km in this particular example, where BER reaches $6.19 \cdot 10^{-12}$ and Q reaches 6.91 (or 16.789 dB). Besides, FWM peaks appear at lower values of dispersion in fiber, this is why dispersion of 0.4 - 6 ps/nm/km would not interfere with correct detection of the transmitted signal. Figures 11, 12, 13, 14 help to observe a slow signal degradation, but BER is still acceptable here. The signal degrades rapidly at dispersion values of more than 6 ps/nm/km, so it is not possible to detect it correctly. As already noted, FWM phenomenon appears at very low, almost zero values of dispersion, which may be seen in figures 8, 9, where at D = 0 ps/nm/km and D = 0.2 ps/nm/km BER reaches $2.87 \cdot 10^{-4}$ (Q = 3.574) and BER = $2.33 \cdot 10^{-11}$ (Q = 6.675) respectively. The lower dispersion is, the higher FWM appears, therefore it is strongly recommended to use dispersion-shifted fiber cables in optical paths.

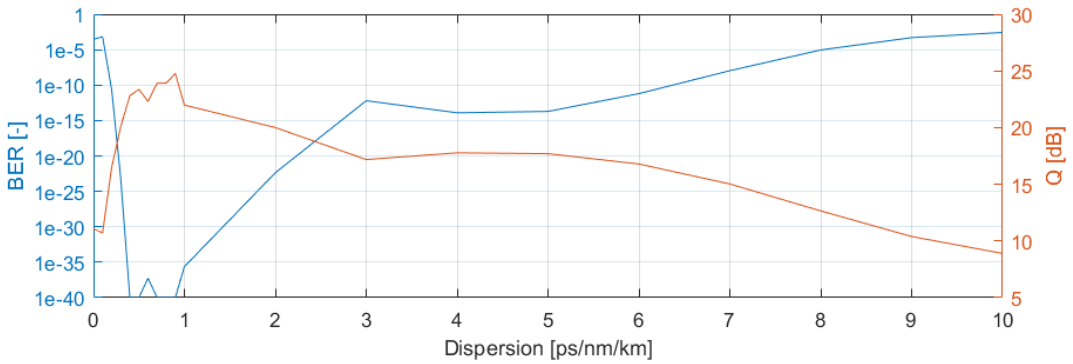

Figure 7: Output signal quality depending on signal dispersion

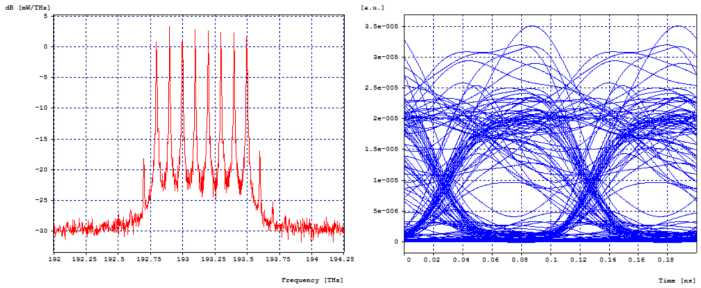

Figure 8: Output FWM and eye diagram with D = 0 ps/nm/km

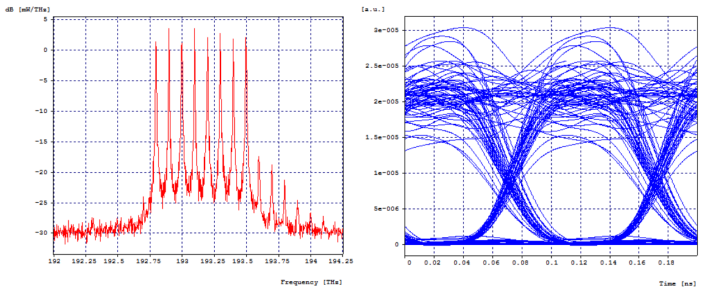

Figure 9: Output FWM and eye diagram with D = 0.2 ps/nm/km

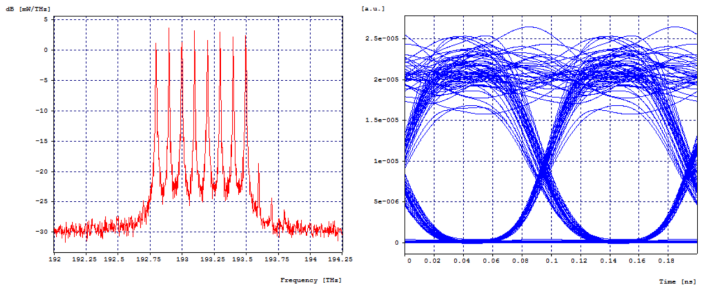

Figure 10: Output FWM and eye diagram with D = 0.3 ps/nm/km

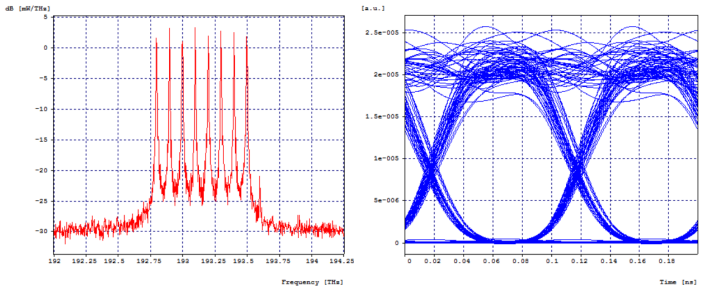

Figure 11: Output FWM and eye diagram with D = 0.4 ps/nm/km

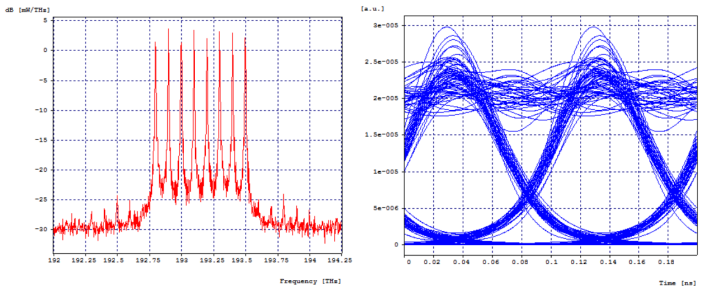

Figure 12: Output FWM and eye diagram with D = 2 ps/nm/km

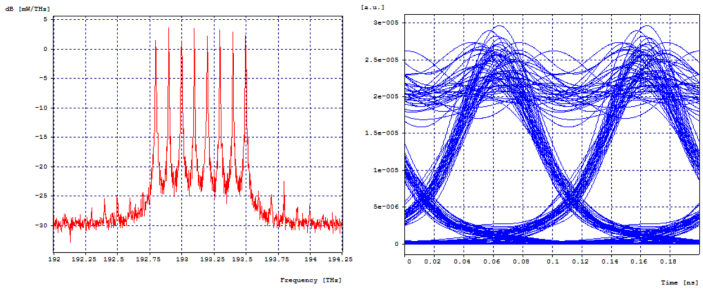

Figure 13: Output FWM and eye diagram with D = 3 ps/nm/km

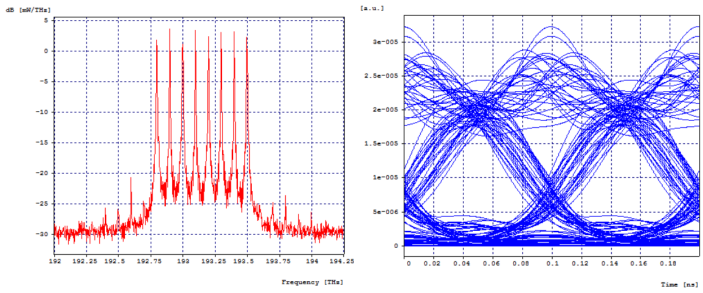

Figure 14: Output FWM and eye diagram with D = 6 ps/nm/km

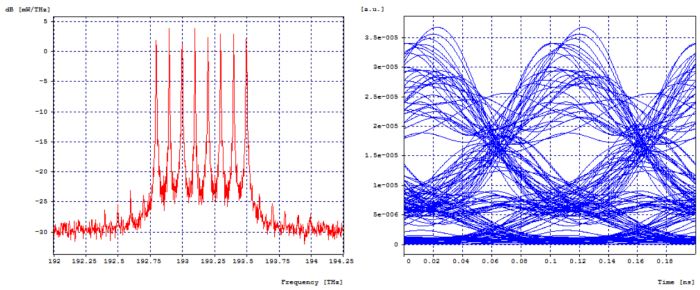

Figure 15: Output FWM and eye diagram with D = 10 ps/nm/km

To draw the conclusion, one can say that FWM decreases when dispersion increases, but simultaneously the signal dissipates, that is why it is important to pick the right dispersion values, which will not lead to generation of lateral signals and keep the signal reliability high, i.e. good BER of output signal. In our case, useful signal in the given optical path is only acquired at D = 0.3 - 6 ps/nm/km (or even 0.3 - 5 ps/nm/km as DWDM systems with capaity over 100 Gbit/s require $BER = 10^{-14}$), although BER reaches the best values (BER = $1 \cdot 10^{-40}$) at D = 0.4 - 0.9 ps/nm/km, which means, that the signal was not distorted during transmission and is still essentially the same as the input signal.

6.2 Output signal depending on input signal power

This chapter examines the dependence of output signal quality (parameters BER[-], Q[-], Q[dB]) on input laser power. Since low dispersion values have influence on FWM products creation, it was set to D = 5 ps/nm/km in this experiment, i.e. the value which does not cause FWM effect and still allows good BER of the transfered signal (see tab.1). Laser power was being chaged from -10 dBm to 10 dBm (from -5 dBm to 10 dBm in tab.2). When laser power was set to values from -6 dBm to -10 dBm, BER increased from $2.08 \cdot 10^{-12}$ to $2.047 \cdot 10^{-7}$ respectively. For this reason and also because it makes no sense to use low level of input signal, because using amplifiers leads to greater signal distortion, these values were not included in the table.

The table is followed by Fig.16 representing BER[-] and Q[dB] values depending on fiber dispesion. Pictures of spectral characteristics of output signal, where FWM peaks could be observed, and eye diagram of output signal for certain dispersion are shown below in Fig.16.

Laser power [dBm]	BER [-]	Q[-]	Q[dB]
-5	$1.89 \cdot 10^{-12}$	7.009	16.914
-4	$1.34 \cdot 10^{-14}$	7.695	17.724
-3	$2.20 \cdot 10^{-12}$	7.075	16.995
-2	$1.14 \cdot 10^{-14}$	7.778	17.817
-1	$2.82 \cdot 10^{-15}$	7.820	17.865
0	$1.92 \cdot 10^{-14}$	7.673	17.699
1	$2.46 \cdot 10^{-12}$	7.047	16.960
2	$1.54 \cdot 10^{-13}$	7.442	17.434
3	$4.80 \cdot 10^{-11}$	6.627	16.426
4	$1.94 \cdot 10^{-9}$	6.005	15.571
5	$3.18 \cdot 10^{-8}$	5.386	14.626
6	$4.83 \cdot 10^{-7}$	4.864	13.741
7	$8.54 \cdot 10^{-5}$	3.697	11.358
8	$6.51 \cdot 10^{-4}$	3.140	9.939
9	$3.99 \cdot 10^{-3}$	2.613	8.343
10	$2.85 \cdot 10^{-2}$	2.081	6.367

Table 2: Output signal parameters depending on set laser power

As it seems, it is possible to separate useful signal from created FWM products by increasing laser power, which is shown in Figs.21, 22, 23, 24, 25, where P_{Tx} was set to 3 dBm, 5 dBm, 7 dBm, 10 dBm and 15 dBm respectively. The other side of the coin is, however, that the higher the useful signal level rises above the noise, the worse BER becomes. From these arguments one could conclude, that it is possible to use bigger laser power in order to separate useful signal from noise, but these values should not be too high, so as to avoid input source noise effect on transmitted signal dissipating.

Another hypothesis that can be done from this experiment is that lower values of input signal from laser source cause smaller FWM products generation. Figures 17 - 25 show slow FWM growth while laser power is being increased. The smallest relative power of FWM products is seen when P_{Tx} = -5 dBm. Fig.25 shows disadvantages in this simulation: the peaks have low relative amplitudes even though they were supplied with high additional power.

To conclude, the best output signal quality has been obtained when P_{Tx} was set to values from -5 dBm to 2 dBm, where BER was fluctuating inside limits of $2.82 \cdot 10^{-15}$ [-] (P_{Tx} = -1 dBm) to $2.46 \cdot 10^{-12}$ [-] (P_{Tx} = 1 dBm). The least volumes of FWM products are seen when P_{Tx} = -5 dBm.

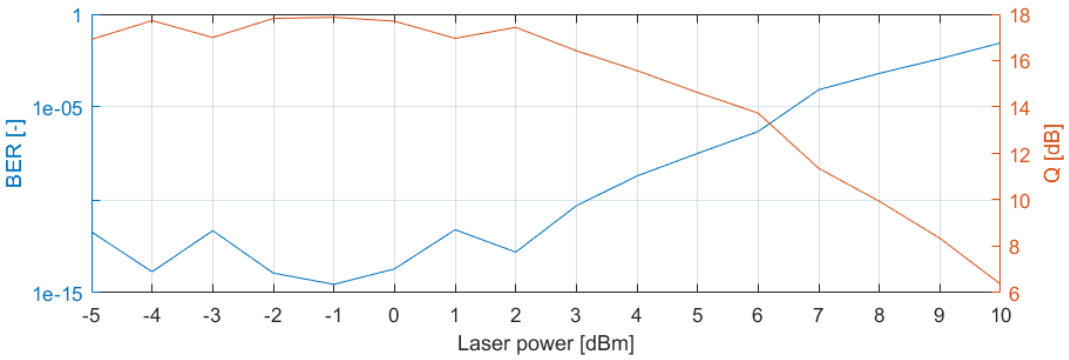

Figure 16: Output signal quality depending on laser power

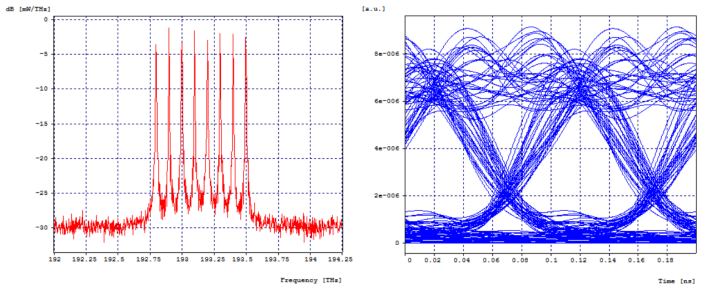

Figure 17: Output FWM and eye diagram with P_{Tx} = -5 dBm, D = 5 ps/nm/km

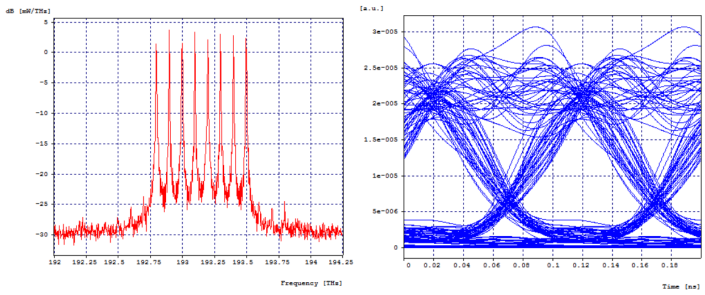

Figure 18: Output FWM and eye diagram with P_{Tx} = 0 dBm, D = 5 ps/nm/km

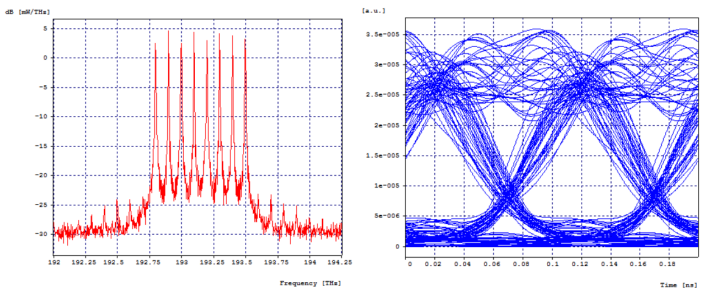

Figure 19: Output FWM and eye diagram with P_{Tx} = 1 dBm, D = 5 ps/nm/km

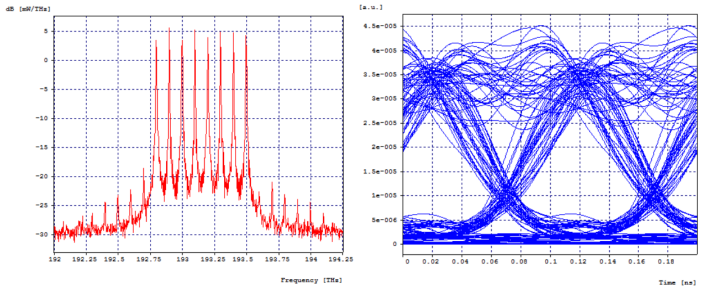

Figure 20: Output FWM and eye diagram with P_{Tx} = 2 dBm, D = 5 ps/nm/km

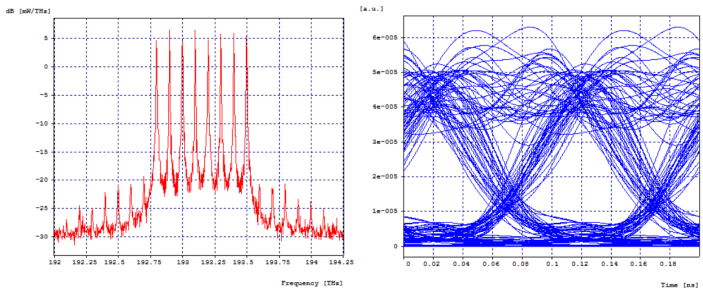

Figure 21: Output FWM and eye diagram with P_{Tx} = 3 dBm, D = 5 ps/nm/km

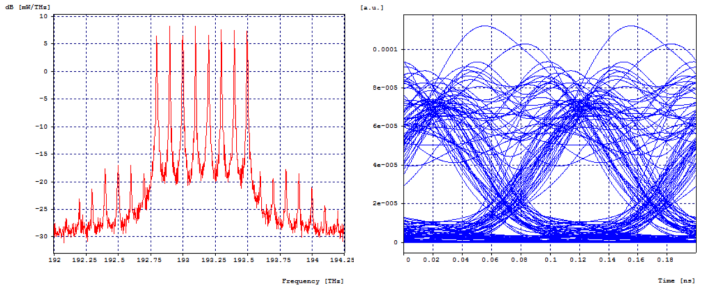

Figure 22: Output FWM and eye diagram with P_{Tx} = 5 dBm, D = 5 ps/nm/km

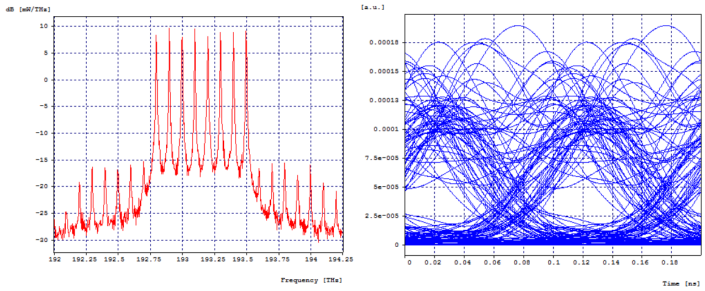

Figure 23: Output FWM and eye diagram with P_{Tx} = 7 dBm, D = 5 ps/nm/km

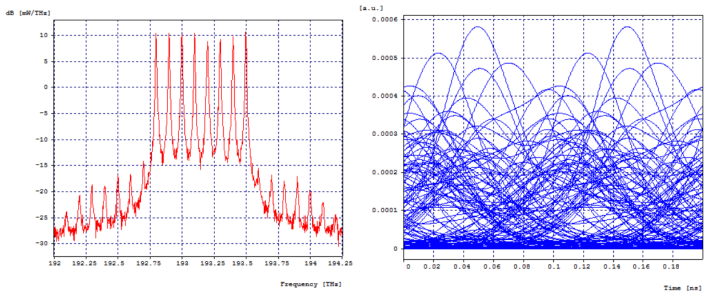

Figure 24: Output FWM and eye diagram with P_{Tx} = 10 dBm, D = 5 ps/nm/km

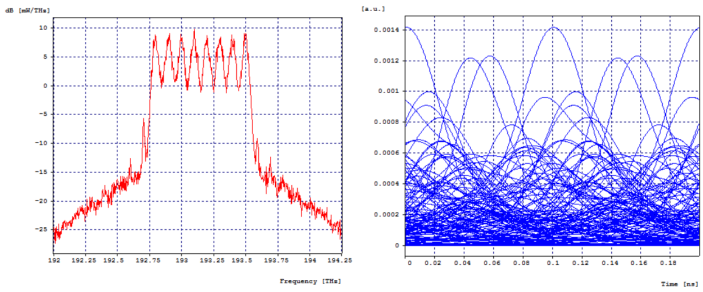

Figure 25: Output FWM and eye diagram with P_{Tx} = 15 dBm, D = 5 ps/nm/km

6.3 Output signal depending both on dispersion in fiber and input signal power

This chapter examines the dependence of output signal quality (parameters BER[-], Q[-], Q[dB]) on input laser power and dispersion in fiber simultaneously. All the results of this experiment are listed in table 3. Dispersion values were taken from the experiment "Output signal depending on signal dispersion in fiber": D = 0 ps/nm/km and D = 0.2 ps/nm/km, i.e. values which lead to maximum FWM production, D = 3 ps/nm/km, where amount of FWM products is smaller, but BER of the signal is good, and D = 6 ps/nm/km, where BER has the last good value in this list (see tab.1). Input signal power was being changed from -5 dBm to 4 dBm, where P_{Tx} = -5 dBm is the value where amount of FWM products is smaller, P_{Tx} = 0, 1, 2 dBm, where BER of the signal is good, P_{Tx} = 3, 4 dBm, where BER of the signal is worse , but FWM products were separated from the useful signal (see tab.2). Parameters BER [-], Q[-], Q[dB] were measured for each combination of dispersion and input laser power values, then there were calculated deterioration ΔQ[%] against P_{Tx} = 0 dBm, as well as deterioration ΔQ5[%] against D = 5 ps/nm/km. Calculated values ΔQ[%] and ΔQ5[%] depending on dispersion in fiber were presented in Figs.26, 27.

D [ps/nm/km]	P_{Tx} [dBm]	BER [-]	Q[-]	Q[dB]	Δ Q[%]	Δ Q5[%]
0	-5	$2.41 \cdot 10^{-16}$	8.126	18.197	+127.36	+15.94
0	0	$2.87 \cdot 10^{-4}$	3.574	11.065	–	-53.42
0	1	$3.68 \cdot 10^{-3}$	2.851	9.100	-20.23	-59.54
0	2	$1.61 \cdot 10^{-2}$	2.202	6.858	-38.39	-70.41
0	3	$3.07 \cdot 10^{-2}$	2.011	6.067	-43.73	-69.65
0	4	$2.27 \cdot 10^{-2}$	2.000	6.021	-44.04	-66.69
0.2	-5	$1.20 \cdot 10^{-28}$	11.069	20.882	+65.83	+57.93
0.2	0	$2.33 \cdot 10^{-11}$	6.675	16.489	–	-13.01
0.2	1	$1.33 \cdot 10^{-7}$	5.205	14.329	-22.02	-26.14
0.2	2	$2.20 \cdot 10^{-5}$	4.086	12.225	-38.79	-45.10
0.2	3	$1.66 \cdot 10^{-3}$	3.068	9.739	-54.04	-53.70
0.2	4	$9.93 \cdot 10^{-3}$	2.361	7.460	-64.63	-60.68
3	-5	$1.20 \cdot 10^{-12}$	6.989	16.888	-3.32	-0.28
3	0	$6.21 \cdot 10^{-13}$	7.229	17.182	–	-5.78
3	1	$1.09 \cdot 10^{-12}$	6.999	16.902	-3.18	-0.68
3	2	$4.41 \cdot 10^{-11}$	6.603	16.395	-8.66	-11.27
3	3	$1.27 \cdot 10^{-11}$	6.673	16.487	-7.69	+0.69
3	4	$5.55 \cdot 10^{-11}$	6.453	16.195	-10.73	+7.46
6	-5	$2.87 \cdot 10^{-9}$	5.862	15.361	-15.17	-16.36
6	0	$6.19 \cdot 10^{-12}$	6.910	16.789	–	-9.94
6	1	$2.33 \cdot 10^{-10}$	6.346	16.049	-8.16	-9.95
6	2	$6.27 \cdot 10^{-9}$	5.861	15.360	-15.18	-21.24
6	3	$1.00 \cdot 10^{-11}$	6.398	16.121	-7.41	-3.45
6	4	$1.00 \cdot 10^{-7}$	5.166	14.263	-25.24	-13.97

Table 3: Output signal parameters depending both on dispersion in fiber and input signal power

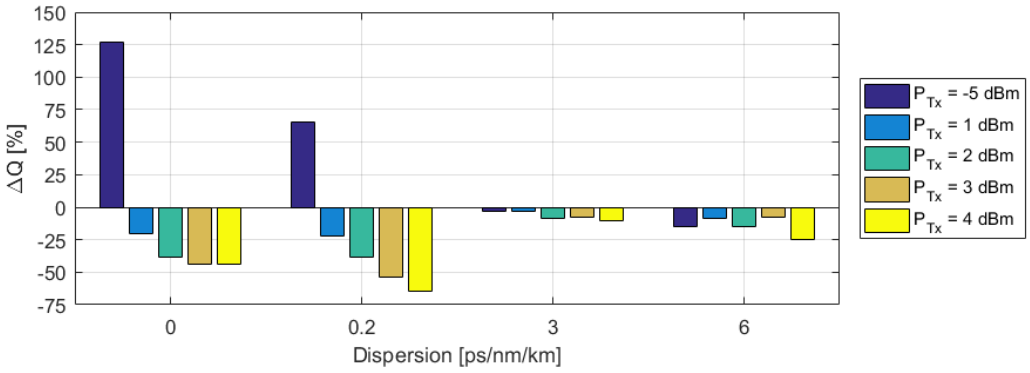

Figure 26: Ratio in % comparison of the Q-factor at specific values of D and P_{Tx} to the values of Q-factor at the $P_{Tx} = 0$ dBm

From Fig.26 above one can draw a conclusion, that when using a fiber with zero- or almost-zero dispersion value, it is better to use the lowest input laser power, in our case P_{Tx} = -5 dBm, where in comparison with D = 0 ps/nm/km there is an obvious improvement in signal (D = 0 ps/nm/km - +127%, D = 0.2 ps/nm/km - +66%). Figures 28, 29 show an example of the fact, that increasing input laser power when using small values of dispersion (D = 0 ps/nm/km, D = 0.2 ps/nm/km), results in significant FWM occurrence, and thus in signal quality deterioration. When using a fiber and dispersion shifted from zero-value, like 3 or 6 ps/nm/km, it is better to set the input laser power to 0 dBm, since the laser power different from this point leads to decrease of signal detection quality. In case when D = 6 ps/nm/km and P_{Tx} = 4 dBm, there is a deterioration of 25%.

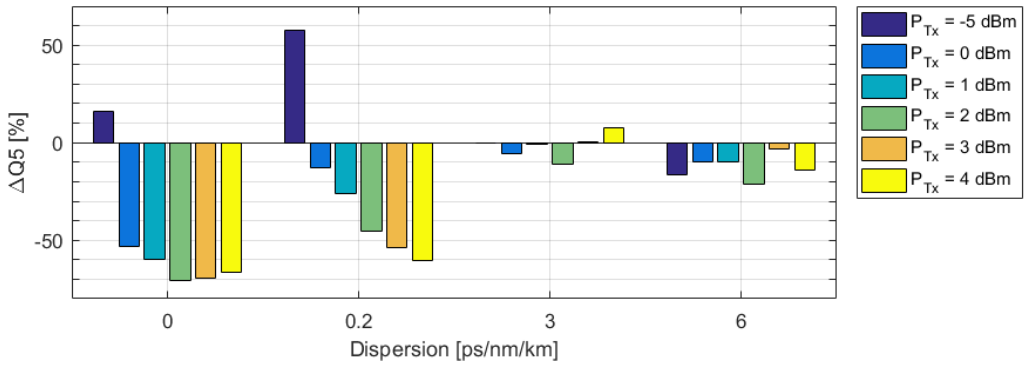

Figure 27: Ratio in % comparison of the Q-factor at specific values of D and P_{Tx} to the values of Q-factor at D = 5 ps/nm/km

From Fig.27 above, where Q of the output signal compares for dispersion 0 and 5 ps/nm/km, 0.2 and 5 ps/nm/km, 3 and 5 ps/nm/km, 6 and 5 ps/nm/km, for each value of input laser power, one can draw a conclusion, that:

- it would be the right choice to set input laser power to P_{Tx} = -5 dBm only in case of using optical fiber with zero or almost-zero dispersion;
- the best option would almost always be (with the exception of the conclusion above) to use dispersion-shifted fibers in optical networks to avoid drastic losses of signal quality, which in this experiment were seen to be of up to 70%.

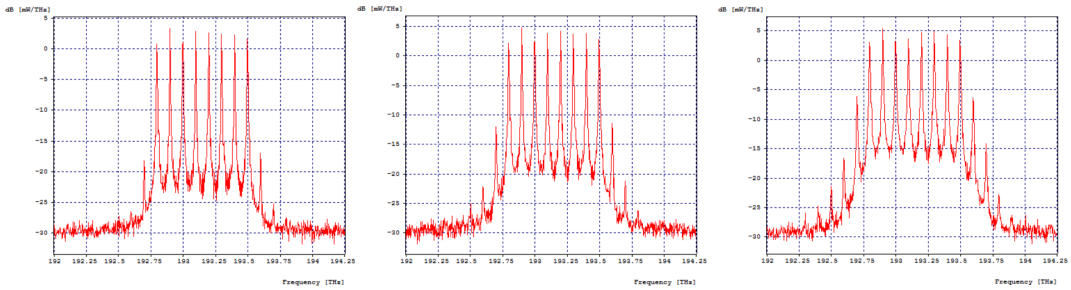

(a) (b) (c)

Figure 28: Output FWM with D = 0 ps/nm/km and P_{Tx} = 0 dBm (a), 2 dBm (b) and 4 dBm (c)

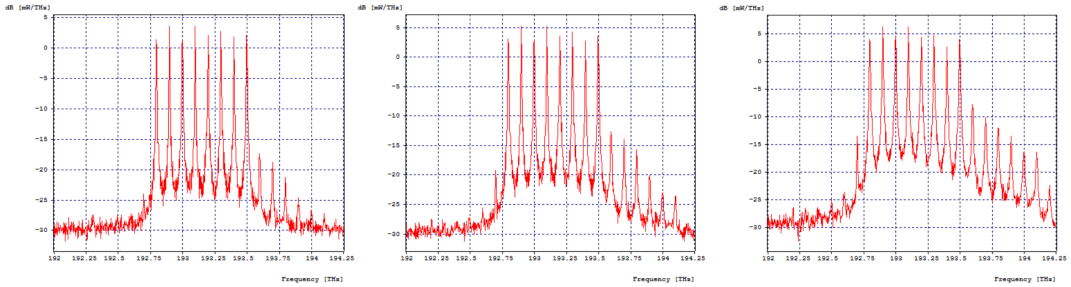

(a) (b) (c)

Figure 29: Output FWM with D = 0.2 ps/nm/km and P_{Tx} = 0 dBm (a), 2 dBm (b) and 4 dBm (c)

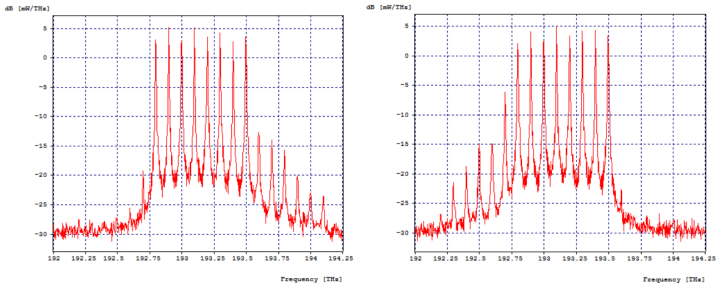

(a) (b)

Figure 30: Comparison of output FWM with P_{Tx} = 2 dBm and D = 0.2 (a) and -0.2 (b) ps/nm/km

Figure 30 illustrates the difference between the use of positive and negative dispersion values - the main FWM products appear, respectively, on higher- and lower-frequency sides of spectrum relatively to the original signal.

6.4 Output signal not influenced by FWM

The main goal of this chapter was to get an output signal by simulation process which would not suffer from FWM phenomenon. For this purpose there was used a circuit which is shown

in figure 31. The components and their parameters are chosen in the way that it could later be compared to practical experiment 8.5.

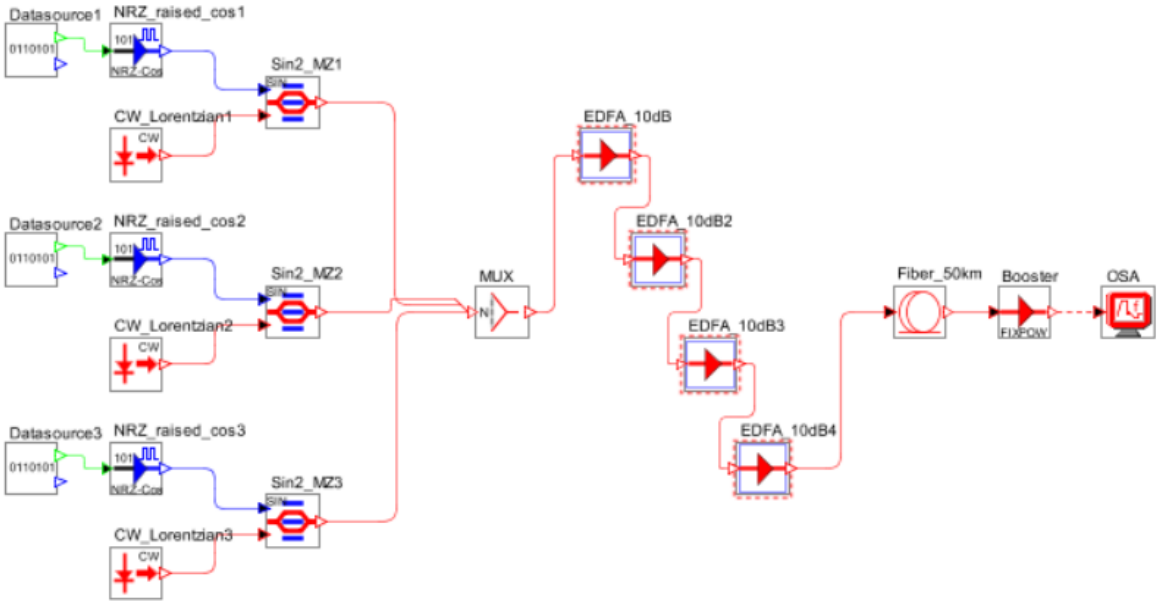

Figure 31: Complete optical path circuit for obtaining an output signal not influenced by FWM phenomenon

The input part of the sircuit is formed by three lasers working on $\lambda_1 = 1530.33$ nm, $\lambda_2 = 1530.725$ nm and $\lambda_3 = 1531.12$ nm, which are then combined by a multiplexor. The whole signal is amplified by 4xEDFA, each of them has a value of 10dB amplification. Amplified signal is bound to a fiber 50km long which a dispersion value 2 ps/nm/km, and then it is amplified again by 11.3dB SOA, so that the gain from all amplifiers is 51.3 dB. The optical path here ends with Optical spectrum analyzer, where the output signal is analyzed.

Another goal in this chapter is to show, that a little change in this circuit, such as dispersion change, or a wrong component order leads to FWM product creation. This is why there were also measured three more possible variants with small changes in the given optical path. The four combinations of the the components order and their parameters are the following:

(a) EDFA – NZDSF, $D = 2$ ps/nm/km – SOA, Fig.33 (a)

(b) EDFA – SOA – NZDSF, $D = 2$ ps/nm/km, Fig. 32, Fig.33 (b)

(c) EDFA – NZDSF, $D = 0$ ps/nm/km – SOA, Fig.33 (c)

(d) EDFA – SOA – NZDSF, $D = 0$ ps/nm/km, Fig. 32, Fig.33 (d)

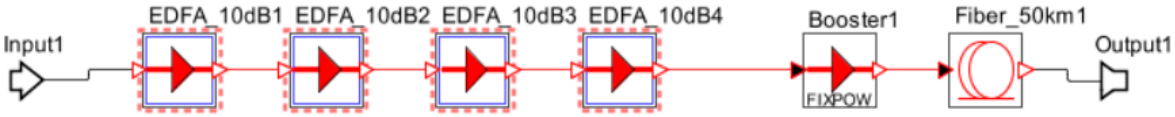

Figure 32: A part of optical path arrangement for raising the non-degenerate FWM phenomenon using three laser sources, a complete circuit may be found in Appendix B

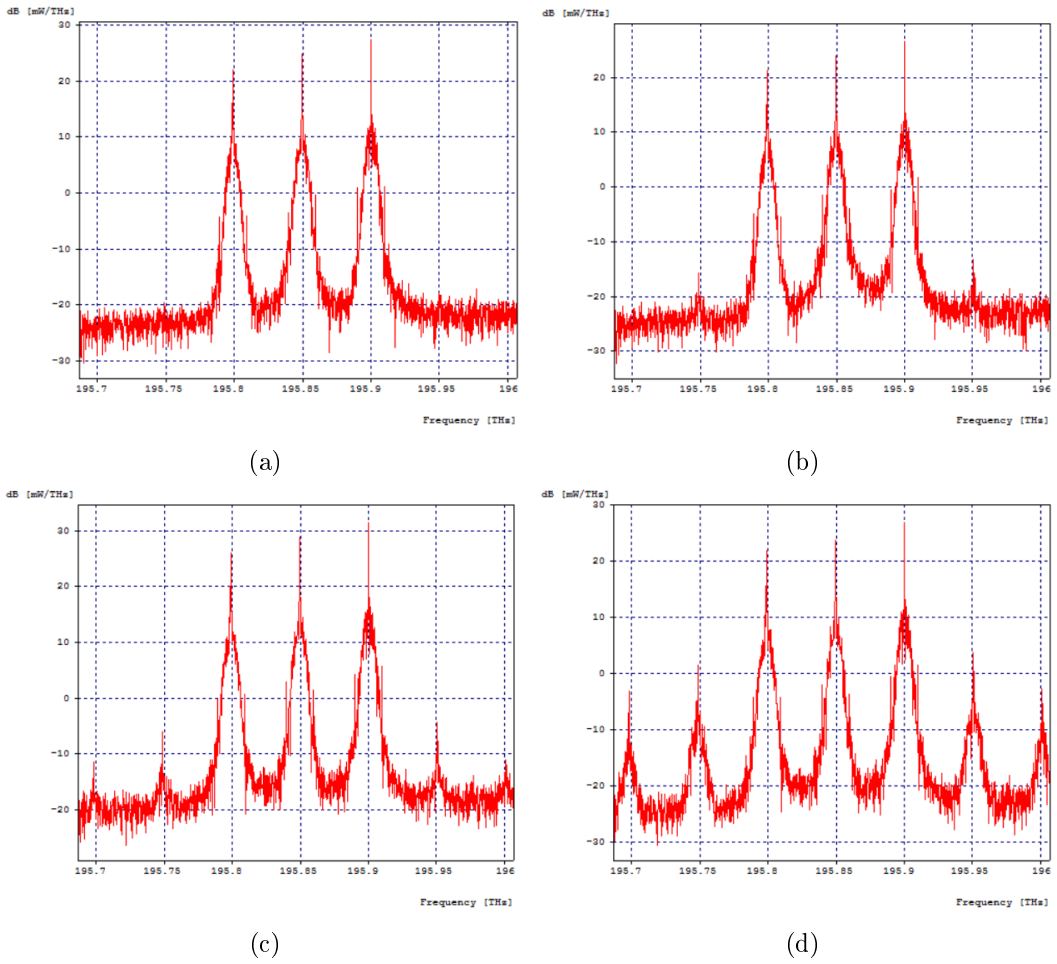

Figure 33: Output signal received from the simulation above (Fig.31), where dispersion and components order is changed according to optical path 32 at a), b) and c)

From the simulation results one can conclude that:

- it is very important to follow all the rules in order to get a pure output signal without FWM products. You can compare Fig.33 (a) where is used a dual-phase amplifier model and a NZDSF fiber, and (d) where dispersion is set on 0 ps/nm/km and a very high amplifier power is set, resulting in the greatest FWM, circuit 32;
- when comparing Fig.33 (b) and (c), a higher FWM power is obtained by zero dispersion than by a wrong components order, or a high power of amplifiers.

7 Precautions when working with optical fiber

One of the most important properties of optical fibers is their bending sensitivity, which shows as attenuation increases in fiber.

When bending optical fiber, the angles of impact and reflection of the transmitted beams change. This may result in a beam exceeding its reflection angle limit and instead of returning to the fiber core it penetrates the shell. The fiber output then receives a lesser number of rays than at the input. At the bending point, the optical fiber is far more prone to damage.

To avoid large bending losses, one should follow the manufacturer's instructions and bend the fiber with the largest possible radius. The smallest bend depends on the diameter of the optical fiber or the cable and on the material from which the fiber is made.

Bends can be classified as macrobendings or microbendings. Based on Fig.34 below, where the influence of macrobending, microbending and basic fiber losses is compared, it can be concluded that it is credible to be guided by precautionary measures regarding the mechanical effect on the optical fiber in order to avoid undesired attenuation increases in the given optical path.

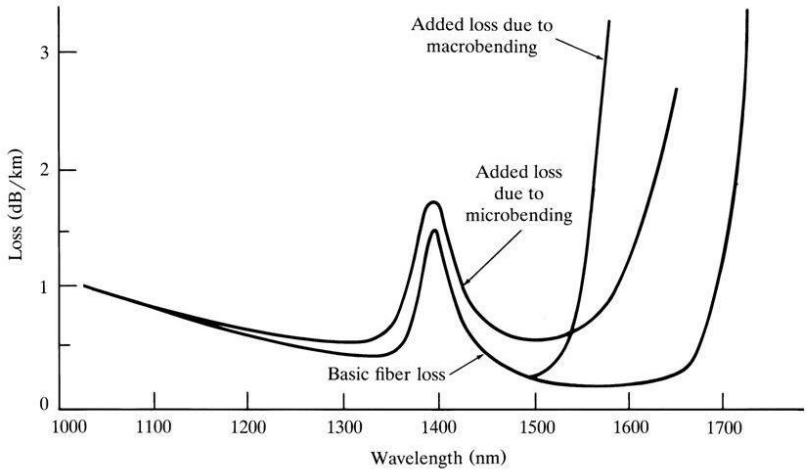

Figure 34: Bending losses in single mode fiber[18]

7.1 Macrobending

When an optical cable is bent not in accordance with the manufacture's instructions, the light cannot be guided along the core of that fibre – thereby resulting in attenuation [25].

The smaller the bending radius is, the more light refracts out of the fiber. In case of single-mode fiber, attenuation also depends on mode field diameter, the difference between

the refractive index of the fiber core and cladding, or index contrast, and the refractive index profile of the fiber.

It follows from the previous sentence, that some steps can be done in order to reduce fiber's sensitivity to macrobendings.

One of them is to change the refractive index profile. Attenuation decreases with refractive index contrast increase. In Figure 35 on the left is shown the macrobending attenuation at 1300 nm for fibers with different numerical apertures (A = 0.253, B = 0.188, C = 0.108). As might have been expected, the attenuation increases exponentially as bend radius decreases, but also greater numerical aperture means higher fiber's sensitivity to macrobendings.

Another way to decrease attenuation caused by macrobendings is to use optical fibers with lower mode field diameter (MFD). Figure 35 on the right compares properties of two different optical fiber cables according to ITU-T Recommendations G.652.D and G.657.A1 with different MFD. Both cables were wrapped in a single 20 mm diameter bend.

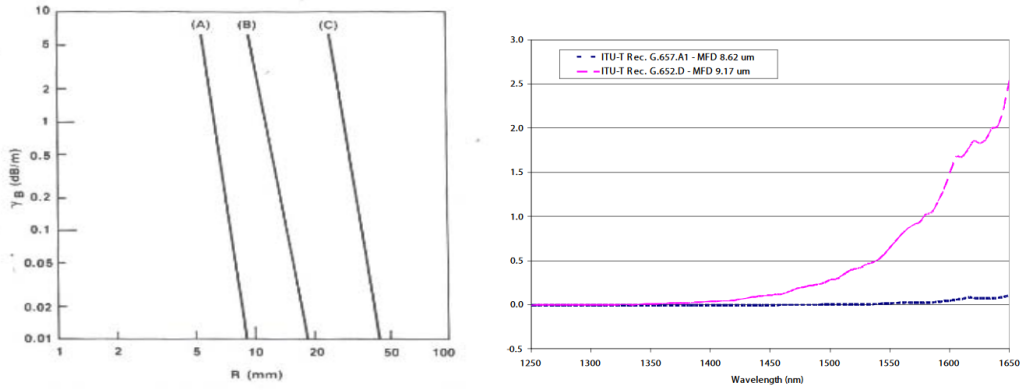

(a) (b)

Figure 35: Influence of refractive index profile (a) and mode field diameter (b) on fiber's sensitivity to macrobendings [36]

7.2 Microbending

Microbendings are distortions of fiber linearity and small errors in fiber geometry. Such deformations have a wide range of potential causes. The physical cause of the perturbations is usually assumed to be due to radial cpmpression of the fiber, or lateral contact of the fiber with other surfaces. They also may appear during the manufacture of the fiber.

When meeting a microbending, some beams are reflected at a large angle, escaping from the core of the optical fiber and increasing its attenuation.

The micro-bends may be very localised, affecting only millimetres of optical fibre length, but producing very large losses up to 40 dB.

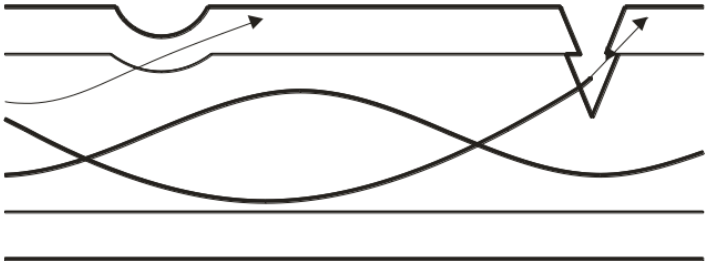

Figure 36: Microbending losses [25]

7.3 Optical connectors upkeep

For the proper operation of the optical network, it is essential that the insertion loss of each component is as low as possible. In most cases the cause of increased attenuation is the contamination of the ferrule of optical connectors. Common light contamination, such as grease after contact with human skin, or slight dusting, can usually be just wiped off, but to make sure that none of it creates additional attenuation, it is recommended to clean them with isopropyl, compressed air and special microfiber cloths.

8 Practical experiments

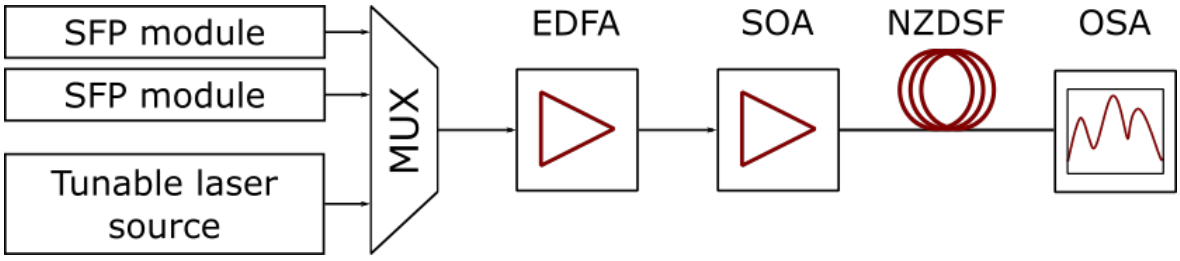

Figure 37: Complete optical path arrangement for FWM generation

This part of the thesis is dedicated to creation of FWM through laboratory experiment. It is possible to reach FWM using a correct (or incorrect, since FWM is an undesirable effect) combination of components, their positions, and set parameters.

The whole experiment oriented on FWM generation was conducted using the circuit as is in figure 37. The output part is made of two Small Form-Factor Pluggable Transceiver (SFP) modules by RLC plugged into a HP V1910-16G Switch [6] and transmitting signals on $\lambda_1 = 1530.33$ nm (= 195.841 THz) and $\lambda_3 = 1531.12$ nm (= 195.740 THz) (see their spectrum in figure 38(a)), and a Tunable optical laser FLS-2600B by EXFO [5], [3] (in figure 38(b) with set $\lambda_2 = 1530.725$ nm). All three lasers had the default power of 0 dbm. In figure 38(b) it is clearly seen how this tunable laser has a very narrow spectral width relative to the static lasers, and in Fig.39 we can also see its optical 3 dB bandwidth, which is just 0.45 nm.

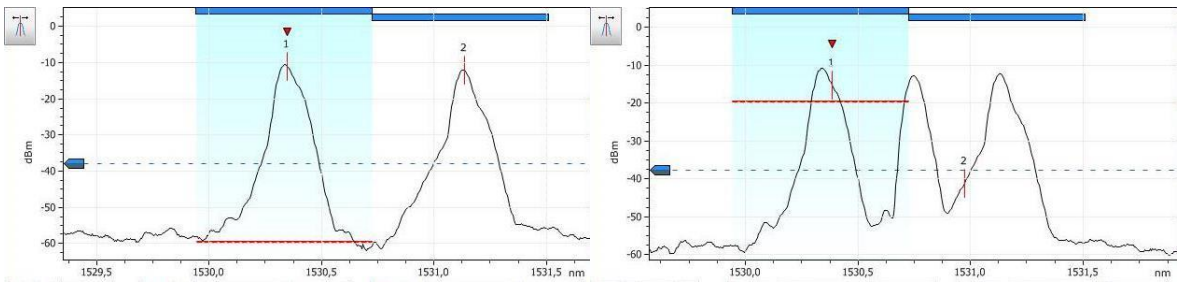

(a) (b)

Figure 38: a) SFP modules spectrum, b) spectrum of all three lasers together

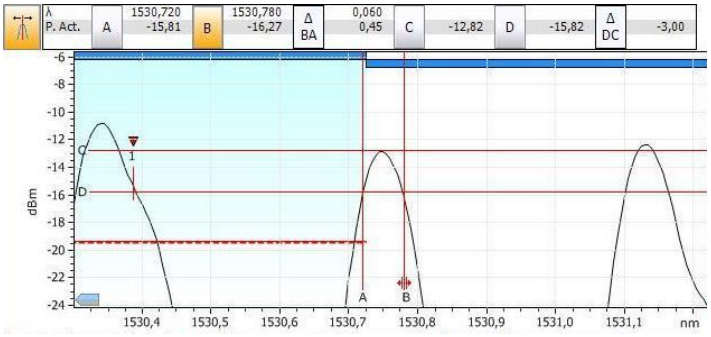

Figure 39: Tunable laser optical 3dB bandwidth

Signal is coupled using a MUX unit, and is then amplified with Erbium doped fiber amplifier by IDIL fibres optiques [1] and Semiconductor optical amplifier S7FC1013S by THORLABS [7].

Electric current through the amplifier's pump in EDFA is set to 156mA, which means the maximum amplification for used EDFA unit. Figure 40(a) illustrates EDFA's gain in a wide spectrum covering the C-band, that is ranged from 1530nm to 1565nm, and L-band with wavelength range from 1570nm to 1610nm. Maximum gains for C-band and L-band are 47dB and 40dB respectively. The minimum gain for used EDFA is 30dB. This setup is optimal if the useful signal is sent over C-band. In case that the signal is being sent over L-band, amplifiers with longer doped fiber with higher pump power should be used [9]. Figure 40(b) illustrates EDFA's gain on wavelengths 1530.33nm and 1531.12nm, marked with A and B, which equals approximately 44.3dB.

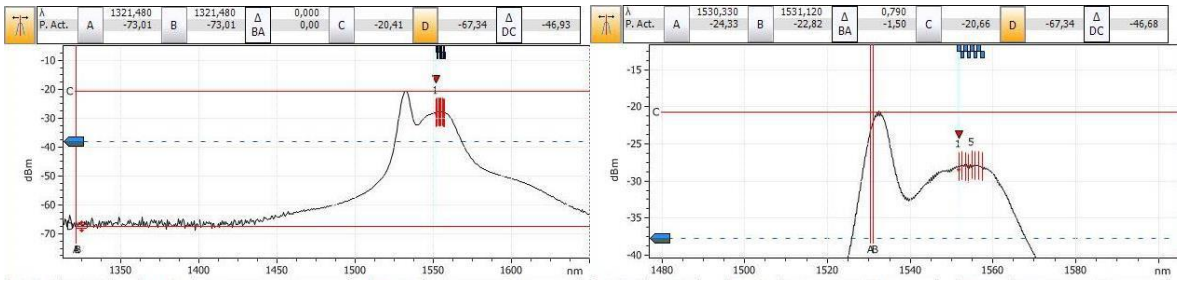

(a) (b)

Figure 40: a) EDFA gain over the whole band, b) EDFA gain on main used wavelengths

SOA has also the power set on maximum, that is 500mA. Figure 41 demonstrates the SOA's gain over the whole band, with maximum on approximately 8dB. Figure 42 demonstrates this band in a more detailed way with (a) showing its optical 3dB bandwidth stretching over 92nm and (b) showing the gain between the main used wavelengths $\lambda_1 = 1530.33$ nm and $\lambda_3 = 1531.12$ nm, that is around 7dB. That means both amplifiers generate gain of 51.3dB.

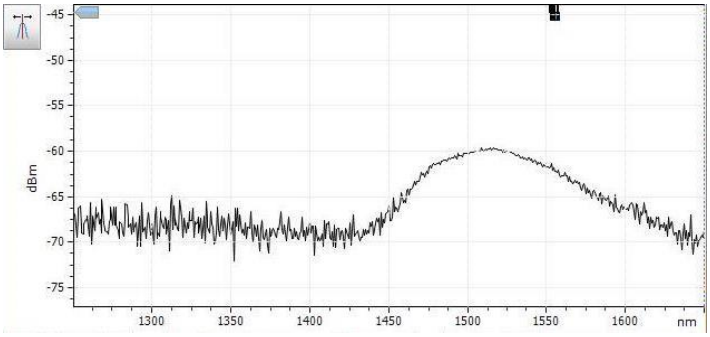

Figure 41: SOA gain over the whole band

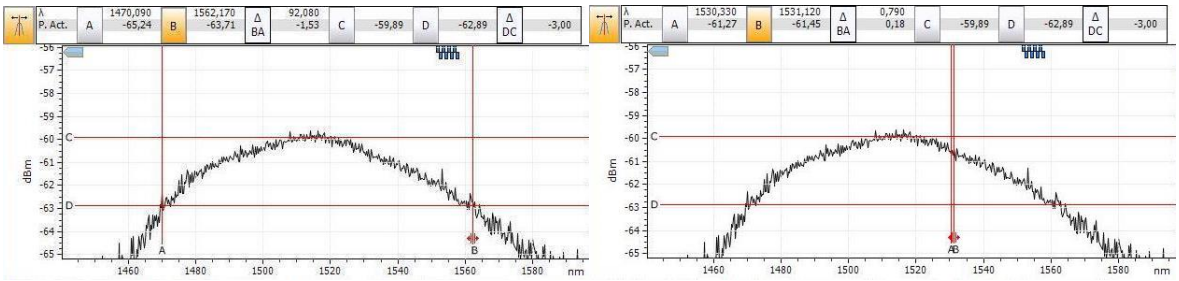

(a) (b)

Figure 42: a) SOA optical 3dB bandwidth, b) SOA gain on main used wavelengths

Amplified signal is bound to a NZDSF fiber 50km long with dispersion of 2 ps/nm/km. Information about different types of fibers regarding their dispersion can be found in section 3.2. The optical path here ends with Optical spectrum analyzer FTB-500 by EXFO [4], where the output signal is analyzed.

8.1 Measurement of FWM frequencies power depending on their spectral shift due to one of three lasers gradual spectral position shift

This experiment was set accordingly to the layout shown in figure 37: input included three lasers - two static during the whole experiment at $\lambda_{las1} = 1530.33$nm, $\lambda_{las3} = 1531.12$nm and the tunable one with λ_{las2} going from 1530.43nm to 1531.03nm (from $\lambda_{las1} + 0.1$nm to $\lambda_{las3} - 0.1$nm) with a step of 0.1 nm.

Following the gradual change of dynamic laser's spectral position, FWM products' spectral positions also changed as shown in table 4 below on the left, where first row shows the spectral positions of second laser and values below show positions of each of nine FWM product.

Table 5 shows FWM products' powers measured for all seven combinations of three channels. Tecnically, in every case we should have seen nine FWM peaks but some of them were hidden underneath useful signals and therefore could not be measured. It is important to remember that the worst situation happens when all the channels are spaced equally far apart, in this case $\lambda_{las2} = \lambda_{las1} + 0.4$nm, so that five out of nine FWM products fall exactly under useful signals.

The aforementioned two tables were compared and merged in graph 43 in a way that close wavelengths from both tables were matched and then measured values were given index numbers $\lambda_1 - \lambda_9$. Although because of some values missing, namely the ones hiding inside useful signals, not all FWM products have a complete set of corresponding values. Therefore λ_2 and λ_6 as the ones not having enough plot points were completely excluded from the graph. All the rest of the wavelengths were presented in Fig.43. Even though some of these wavelengths were also incomplete, they are still present in the graph because the curves' behaviour is still easily observed.

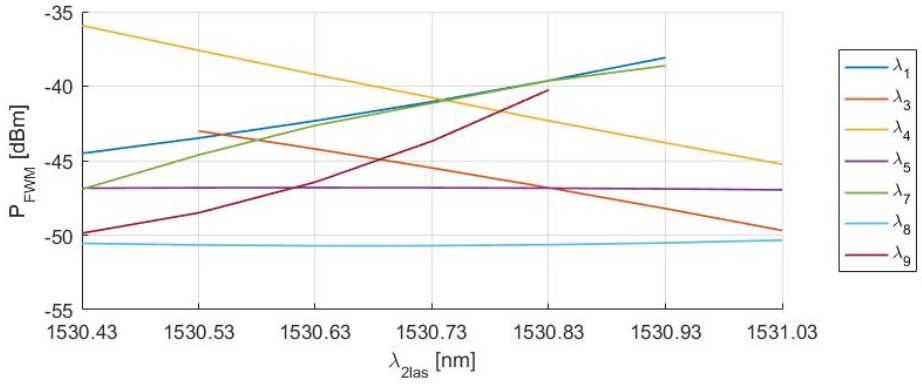

Figure 43: Changes of FWM products power depending on their spectral positions

It is obvious from the graph that two of the FWM wavelengths which did not change their spectral positions, namely λ_5 and λ_8, were also static in the means of their power, since these two wavelengths are only dependent on lasers λ_{las1} and λ_{las3} ($\lambda_5 = 2\lambda_i - \lambda_k$, $\lambda_8 = 2\lambda_k - \lambda_i$). Based on this observation it can be assumed that considering constant laser power FWM

λ_{FWM}	$\lambda_{las1}+0.1$[nm]	$\lambda_{las1}+0.2$[nm]	$\lambda_{las1}+0.3$[nm]	$\lambda_{las1}+0.4$[nm]	$\lambda_{las1}+0.5$[nm]	$\lambda_{las1}+0.6$[nm]	$\lambda_{las1}+0.7$[nm]
	1530.43	1530.53	1530.63	1530.73	1530.83	1530.93	1531.03
$\lambda_1=\lambda_i+\lambda_j-\lambda_k$	1529.64	1529.74	1529.84	1529.94	1530.04	1530.14	1530.24
$\lambda_2=\lambda_i-\lambda_j+\lambda_k$	1531.02	1530.92	1530.82	1530.72	1530.62	1530.52	1530.42
$\lambda_3=\lambda_j+\lambda_k-\lambda_i$	1531.22	1531.32	1531.42	1531.52	1531.62	1531.72	1531.82
$\lambda_4=2\lambda_i-\lambda_j$	1530.23	1530.13	1530.03	1529.93	1529.83	1529.73	1529.63
$\lambda_5=2\lambda_i-\lambda_k$	1529.54	1529.54	1529.54	1529.54	1529.54	1529.54	1529.54
$\lambda_6=2\lambda_j-\lambda_i$	1530.53	1530.73	1530.93	1531.13	1531.33	1531.53	1531.73
$\lambda_7=2\lambda_j-\lambda_k$	1529.74	1529.94	1530.14	1530.34	1530.54	1530.74	1530.94
$\lambda_8=2\lambda_k-\lambda_i$	1531.91	1531.91	1531.91	1531.91	1531.91	1531.91	1531.91
$\lambda_9=2\lambda_k-\lambda_j$	1531.81	1531.71	1531.61	1531.51	1531.41	1531.31	1531.21

Table 4: Table of spectral positions of received FWM products depending on the set three lasers frequencies (on the left) and a preview of spectral positions of FWM products and useful channels for $\lambda_{las2}=\lambda_{las1}+0.1$nm (on the right)

λ_{las2}[nm]	№$_{pr.}$	λ_{FWM}[nm]	P_{FWM}[dBm]	λ_{las2}[nm]	№$_{pr.}$	λ_{FWM}[nm]	P_{FWM}[dBm]
λ_{las1}+0.1	1	1529.55	-46.72	λ_{las1}+0.2	1	1529.54	-47.05
	2	1529.67	-44.32		2	1529.77	-43.87
	3	1529.77	-46.32		3	1529.99	-45.24
	4	1530.23	-35.99		4	1530.13	-37.71
	5	1531.80	-49.88		5	1530.75	-40.63
	6	1531.92	-50.54		6	1530.93	-40.98
					7	1531.34	-43.04
					8	1531.70	-48.32
					9	1531.93	-50.75
λ_{las2}[nm]	№$_{pr.}$	λ_{FWM}[nm]	P_{FWM}[dBm]	λ_{las2}[nm]	№$_{pr.}$	λ_{FWM}[nm]	P_{FWM}[dBm]
λ_{las1}+0.3	1	1529.54	-46.78	λ_{las1}+0.4	1	1529.55	-46.79
	2	1529.87	-42.62		2	1529.95	-39.79
	3	1530.01	-38.83		3	1531.51	-43.21
	4	1530.16	-43.38		4	1531.92	-50.61
	5	1530.81	-42.13				
	6	1531.44	-45.08				
	7	1531.61	-46.94				
	8	1531.91	-50.66				
λ_{las2}[nm]	№$_{pr.}$	λ_{FWM}[nm]	P_{FWM}[dBm]	λ_{las2}[nm]	№$_{pr.}$	λ_{FWM}[nm]	P_{FWM}[dBm]
λ_{las1}+0.5	1	1529.55	-46.77	λ_{las1}+0.6	1	1529.54	-46.89
	2	1529.81	-42.64		2	1529.71	-43.81
	3	1530.07	-40.68		3	1530.17	-37.80
	4	1530.59	-37.90		4	1530.78	-39.60
	5	1531.39	-40.41		5	1531.56	-49.32
	6	1531.64	-48.19		6	1531.74	-48.72
	7	1531.92	-50.61		7	1531.92	-50.76
λ_{las2}[nm]	№$_{pr.}$	λ_{FWM}[nm]	P_{FWM}[dBm]				
λ_{las1}+0.7	1	1529.54	-47.00				
	2	1529.61	-45.14				
	3	1531.77	-49.60				
	4	1531.84	-49.20				
	5	1531.91	-50.22				

Table 5: Measured power values of FWM frequencies depending on their spectral position

product would only change its power if it changes its spectral position. Also it can be noticed that powers of the rest of FWM wavelengths either were constantly rising or constantly declining. According to illustration 4 on the right, the rising wavelengths (λ_1, λ_7, λ_9) are located near the ends of the observed spectrum band and are travelling towards the middle of the spectrum, meanwhile the declining wavelengths are those travelling in direction opposite from the middle. From all those observations one can draw a conclusion that FWM products travelling away from the laser channels give away their energy to those FWM products travelling opposite directions.

8.2 Comparison of measured FWM values with the calculated values

The following experiment was set in a completely same way as in subsection 8.1, but this time the emphasis was put on FWM products' spectral positions instead of their powers.

The measurement was conducted for two lasers static during the whole experiment at $\lambda_{las1} = 1530.33$nm, $\lambda_{las3} = 1531.12$nm and the tunable one with $\lambda_{las2} = \lambda_{las1} + 0.3$nm (tab.6 on the left), $\lambda_{las2} = \lambda_{las1} + 0.4$nm (tab.7 on the left), $\lambda_{las2} = \lambda_{las1} + 0.5$nm (tab.8 on the left).

Measured FWM frequencies were then compared to the teoretically calculated according to equations shown in tables 6, 7, 8 on the left and are put on pictures to the right from said tables with red arrows meaning the calculated frequencies.

In case of $\lambda_{las2} = \lambda_{las1} + 0.4$nm inside of every useful signal channel there happened to be one of FWM products with their spectral centers perfectly aligned, and therefore said parasitic frequencies have their biggest possible powers. Other cases where channel spacing was uneven, had FWM products occurring unaligned with useful signal, which made them both weaker and easier to filter out. From the above analysis it is possible to conclude that during planning the DWDM systems it is ill-advised to put all the channels evenly spaced away from each other unless the set up in question has no FWM at all.

equation	λ_n	λ_{FWM}[nm]
$\lambda_i + \lambda_j - \lambda_k$	λ_1	1529.84
$\lambda_i - \lambda_j + \lambda_k$	λ_2	1530.82
$\lambda_j + \lambda_k - \lambda_i$	λ_3	1531.42
$2\lambda_i - \lambda_j$	λ_4	1530.03
$2\lambda_i - \lambda_k$	λ_5	1529.54
$2\lambda_j - \lambda_i$	λ_6	1530.93
$2\lambda_j - \lambda_k$	λ_7	1530.14
$2\lambda_k - \lambda_i$	λ_8	1531.91
$2\lambda_k - \lambda_j$	λ_9	1531.61

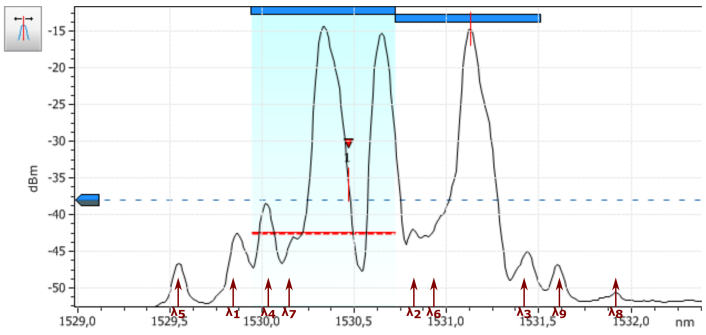

Table 6: Calculated spectral positions of FWM products (on the left) and calculated positions compared to measured ones (on the right) for $\lambda_{las2} = 1530.63$nm

equation	λ_n	λ_{FWM}[nm]
$\lambda_i + \lambda_j - \lambda_k$	λ_1	1529.94
$\lambda_i - \lambda_j + \lambda_k$	λ_2	1530.72
$\lambda_j + \lambda_k - \lambda_i$	λ_3	1531.52
$2\lambda_i - \lambda_j$	λ_4	1529.93
$2\lambda_i - \lambda_k$	λ_5	1529.54
$2\lambda_j - \lambda_i$	λ_6	1531.13
$2\lambda_j - \lambda_k$	λ_7	1530.34
$2\lambda_k - \lambda_i$	λ_8	1531.91
$2\lambda_k - \lambda_j$	λ_9	1531.51

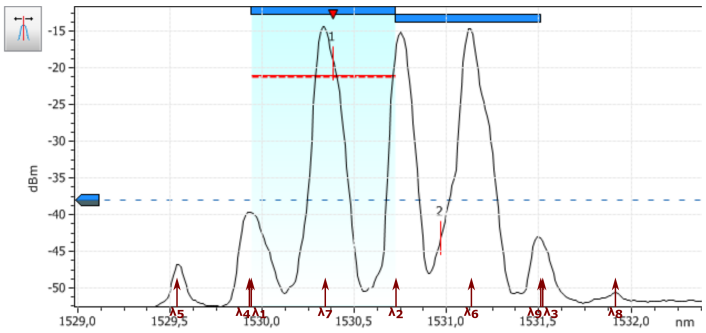

Table 7: Calculated spectral positions of FWM products (on the left) and calculated positions compared to measured ones (on the right) for $\lambda_{las2} = 1530.73$nm

equation	λ_n	λ_{FWM}[nm]
$\lambda_i + \lambda_j - \lambda_k$	λ_1	1530.04
$\lambda_i - \lambda_j + \lambda_k$	λ_2	1530.62
$\lambda_j + \lambda_k - \lambda_i$	λ_3	1531.62
$2\lambda_i - \lambda_j$	λ_4	1529.83
$2\lambda_i - \lambda_k$	λ_5	1529.54
$2\lambda_j - \lambda_i$	λ_6	1531.33
$2\lambda_j - \lambda_k$	λ_7	1530.54
$2\lambda_k - \lambda_i$	λ_8	1531.91
$2\lambda_k - \lambda_j$	λ_9	1531.41

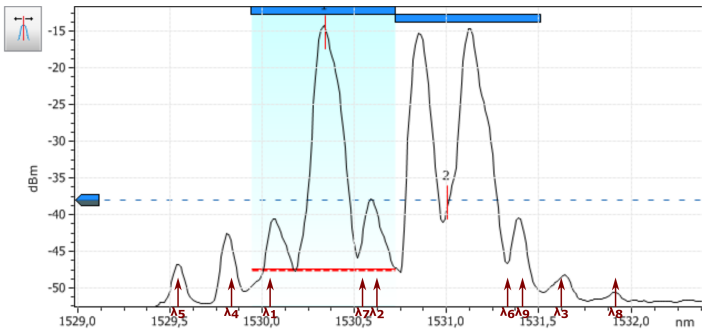

Table 8: Calculated spectral positions of FWM products (on the left) and calculated positions compared to measured ones (on the right) for $\lambda_{las2} = 1530.83$nm

8.3 Output signal dependence on input laser power

This experiment was again set accordingly to the layout shown in Fig.37: input included three lasers - two static during the experiment at $\lambda_{las1} = 1530.33$nm, $\lambda_{las3} = 1531.12$nm and the tunable one with λ_{las2} going from 1530.63nm to 1531.83nm (from $\lambda_{las1} + 0.3$nm to $\lambda_{las3} - 0.3$nm) with a step of 0.1 nm. But in this case we were also changing input power of the tunable laser from 0 dBm to -5 dBm. Since FWM peaks do not change their positions because of different laser power, it was much easier to locate them. Table 9 has in it all the power values of FWM products that could have been seen - the ones not hidden behind useful signals, depending on input laser power for $\lambda_{las2} = \lambda_{las1} + 0.3$ nm, $\lambda_{las2} = \lambda_{las1} + 0.4$ nm, $\lambda_{las2} = \lambda_{las1} + 0.5$ nm. Since the use of all three frequencies led to very similar results, only the option with $\lambda_{las2} = \lambda_{las1} + 0.3$ nm was used to generate graph 45 of FWM peaks power dependency on input laser power. As seen in figure 44 only seven FWM peaks are visible and therefore graph 45 only has seven curves. Let it be noted that Y asis in graph 45 does not display absolute powers of each FWM product, but instead has their change of power relative to their own previous value, which is why X axis starts at 1 dBm instead of 0 dBm where measurement began.

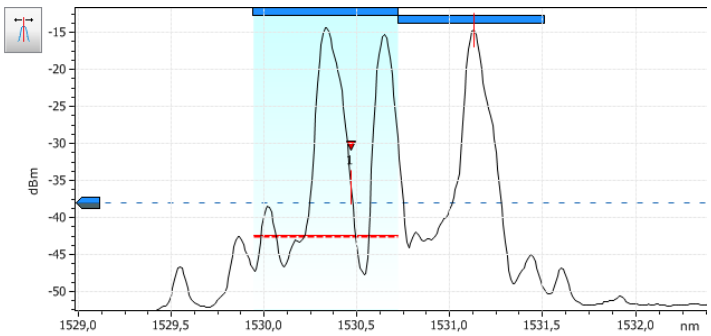

Figure 44: Example of spectrum used to make graph 45

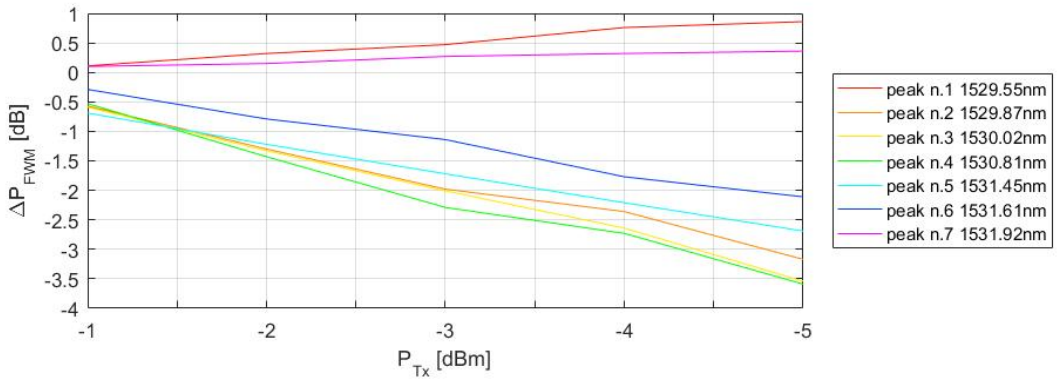

Figure 45: FWM power depending on input laser power

$\Lambda_{tun.laser}$	№	Λ_{FWM} [nm]	P_{FWM} [dBm] for $P_{Tlaser}=$ 0dBm	P_{FWM} [dBm] for $P_{Tlaser}=$ -1dBm	P_{FWM} [dBm] for $P_{Tlaser}=$ -2dBm	P_{FWM} [dBm] for $P_{Tlaser}=$ -3dBm	P_{FWM} [dBm] for $P_{Tlaser}=$ -4dBm	P_{FWM} [dBm] for $P_{Tlaser}=$ -5dBm
Λ_{laser1}+0.3 nm = 1530.63 nm	1	1529.55	-46.69	-46.58	-46.37	-46.22	-45.93	-45.83
	2	1529.87	-42.44	-43.01	-43.74	-44.42	-44.8	-45.61
	3	1530.02	-38.47	-39.06	-39.80	-40.48	-41.11	-42.01
	4	1530.81	-41.82	-42.35	-43.25	-44.11	-44.55	-45.41
	5	1531.45	-45.05	-45.74	-46.27	-46.77	-47.26	-47.74
	6	1531.61	-47.00	-47.29	-47.79	-48.14	-48.77	-49.11
	7	1531.92	-50.67	-50.57	-50.52	-50.4	-50.35	-50.31
Λ_{laser1}+0.4 nm = 1530.73 nm	1	1529.55	-46.83	-46.61	-46.34	-46.11	-46.00	-45.84
	2	1529.93	-39.70	-40.16	-40.63	-41.61	-42.35	-43.06
	3	1531.50	-43.31	-43.82	-44.22	-44.99	-45.45	-46.02
	4	1531.91	-50.71	-50.63	-50.54	-50.42	-50.38	-50.33
Λ_{laser1}+0.5 nm = 1530.83 nm	1	1529.55	-46.91	-46.59	-46.39	-46.12	-45.92	-45.73
	2	1529.82	-42.65	-43.19	-43.77	-44.70	-45.00	-45.76
	3	1530.09	-40.63	-41.31	-41.92	-42.94	-43.46	-44.00
	4	1530.60	-37.69	-38.87	-39.83	-40.76	-41.64	-42.48
	5	1531.40	-40.36	-40.94	-41.68	-42.67	-43.17	-43.99
	6	1531.65	-48.35	-48.66	-49.02	-49.26	-49.46	-49.84
	7	1531.92	-50.63	-50.46	-50.38	-50.27	-50.13	-50.23

Table 9: Output FWM power depending on input laser power

From the graph it can be observed that some of those peaks exhibit increase in power while others showed the decrease. By checking the spectrum we can see that the FWM peaks that increase their power with decreasing input laser power are located far away from useful signal, while those FWM peaks located close around weaken with decrease of input laser power. Therefore it is recommended using weaker input power in order to decrease the more inconvenient FWM products.

8.4 Degenerate FWM

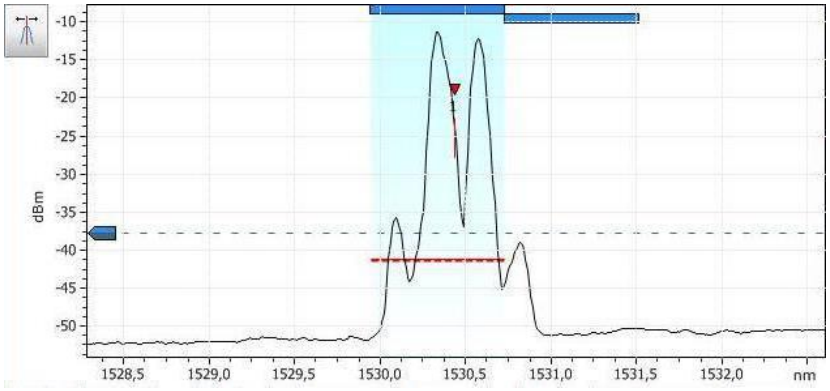

Figure 46: Degenerate FWM for $\Delta\lambda_{ij}$=0.25 nm

$\Delta\lambda_{ij}$[nm]	λ_j[nm]	P_{FWM1}[dBm]	P_{FWM2}[dBm]
0.25	1530.58	-35.81	-38.95
0.30	1530.63	-35.61	-39.25
0.35	1530.68	-37.33	-42.43
0.40	1530.73	-37.76	-43.58
0.45	1530.78	-39.94	-46.28
0.50	1530.83	-41.36	-46.93
0.55	1530.88	-42.21	-47.08
0.60	1530.93	-42.21	-47.79
0.65	1530.98	-43.99	—
0.70	1531.03	-45.20	—
0.75	1531.08	-45.90	—
0.80	1531.13	-45.66	—
0.85	1531.18	-46.95	—
0.90	1531.23	-46.90	—
0.95	1531.28	-47.22	—
1.00	1531.33	-47.70	—
1.05	1531.38	-48.17	—

Table 10: Power of FWM products depending on channel spacing

This chapter is about the creation of degenerate FWM which means only two useful signals in the system and therefore only two FWM products. This experiment used almost the same setup as shown in optical path arrangement 37 with the difference being the use of two input lasers instead of three. One of said lasers was statically set on $\lambda_i = 1530.33$ nm, and the second tunable laser's wavelength was being changed from $\lambda_j = 1530.58$ nm to $\lambda_j = 1531.38$ nm with a step of 0.05 nm. The power of FWM products was measured depending on channel spacing until the moment when FWM prodcts were completely lost into noise. The useful channels' powers were unchanged through the course of the experiment. The table 10 represents the dependency of FWM products power on channel spacing; figure 46 demonstrates a definitive case of degenerate FWM with channel spacing of $\Delta\lambda_{ij} = 0.25$ nm.

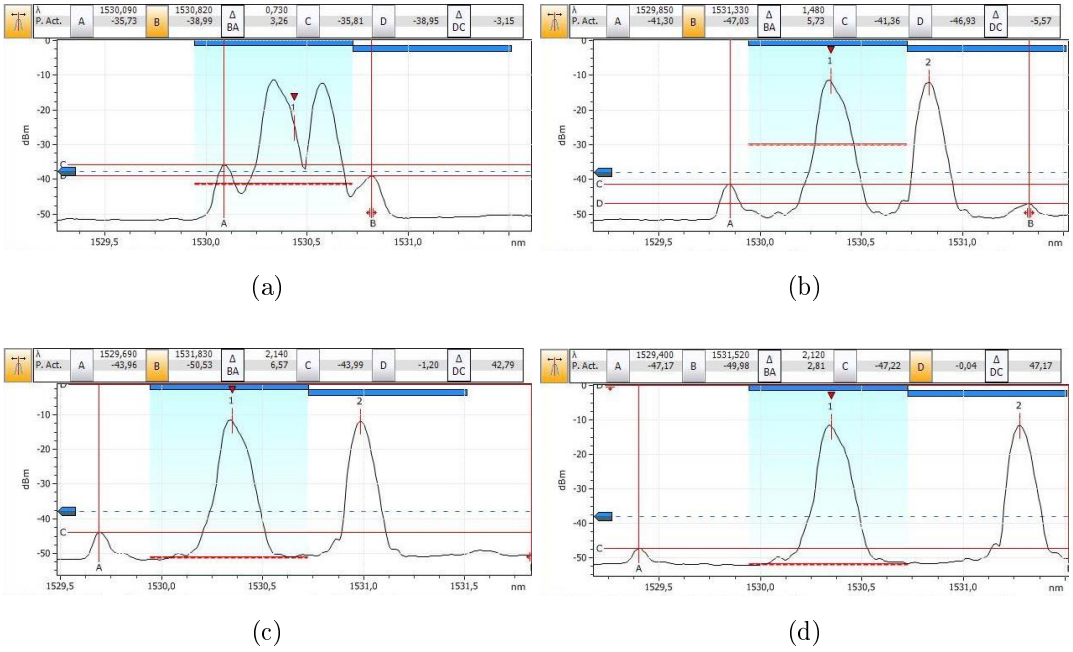

Figure 47: Power of FWM products for a) $\Delta\lambda_{ij}$=0.25 nm, b) $\Delta\lambda_{ij}$=0.5 nm, c) $\Delta\lambda_{ij}$=0.65 nm, d) $\Delta\lambda_{ij}$=1.0 nm

Figure 47 depicts different cases of useful channel positioning and respective FWM products for:

(a) $\Delta\lambda_{ij} = 0.25$ nm - the first measure,

(b) $\Delta\lambda_{ij} = 0.5$ nm,

(c) $\Delta\lambda_{ij} = 0.65$ nm - when the second FWM product is lost to noise and is not any more shown in table 10,

(d) $\Delta\lambda_{ij} = 1.0$ nm - second to the last measurement.

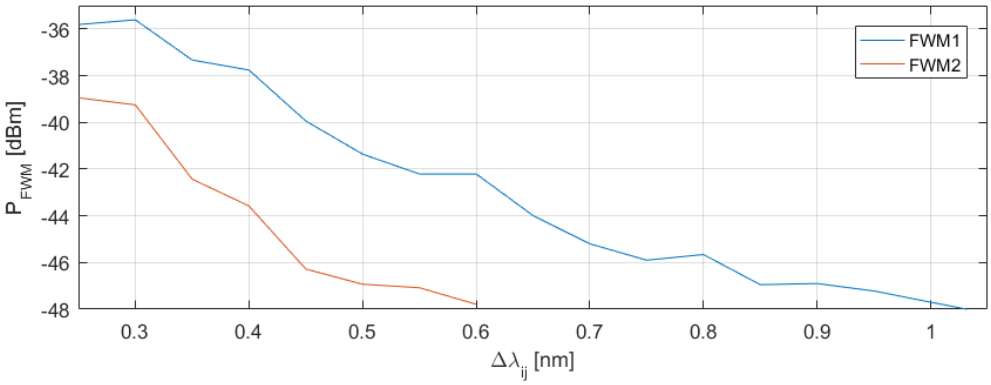

Figure 48: Slow changes of power of two FWM products due to encreasing of channel spacing

Graph 48 demonstrates how exactly does FWM products power decrease with increasing channel spacing, up until the moment when said products are disappeared in noise. It is obvious from the graph that the power of FWM products drops roughly exponentially with increasing channel spacing, with more or less the same speed for both FWM products.

8.5 Output signal unaffected by FWM

The goal of this experiment was to receive an output signal which was not influenced by FWM occurring on the same optical path components. Channel spacing was chosen according to ITU recommendations, which was in our case 0.4 nm. Input laser power was set on 0 dBm, there was also used a NZDSF optical fiber with shifted dispersion, but the output signal in all the experiments carried out before were nevertheless affected by FWM due to high amplifying performance. This is why SOA amplifier and the fiber were swapped here in order to distribute amplifying power to the entire optical network instead of leaving high amplification at one point of the network, which is shown in scheme 49. With application of such a set up, output signal comes out completely unaffected by Four Wave Mixing or any other destructive optical effects, as shown in figure 50.

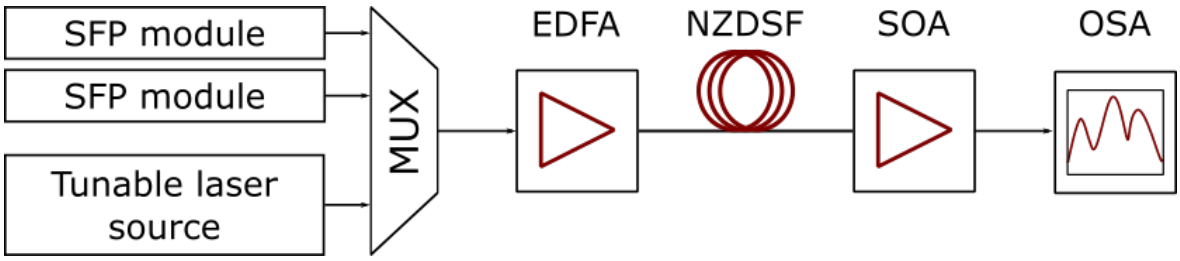

Figure 49: Scheme for achieving an output signal not affected by FWM

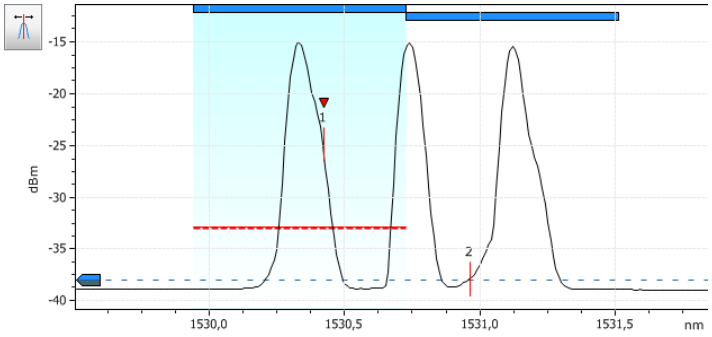

Figure 50: Output signal without FWM products

This model is called dual-phase amplifier, which is strongly recommended to follow in order to receive a good output signal not influenced by FWM.

8.6 Comparison of practically measured and simulated output signal

Figure 51 below represents comparison of measured (a and b) and simulated (c and d) output signal influenced (b and d) and not influenced (a and c) by FWM phenomenon. The circuit parameters for both measurement and simulation non-influenced by FWM variant are:

- three laser sources working on $\lambda_1 = 1530.33$ nm, $\lambda_2 = 1530.725$ nm, $\lambda_3 = 1531.12$ nm;
- power of laser sources 0 dBm;
- dispersion 2 ps/nm/km;
- a dual-phase amplifier model;
- combined maximum gain of all the amplifiers is 51.3 dB.

Only one change was introduced in order to raise the non-degenerate Four Wave Mixing, which is caused by the wrong amplifiers arrangement: a semiconductor amplifier was placed right after an EDFA amplifier.

First and foremost, the OSNR of measured signal without FWM and influenced by FWM is the same: 23 dB for simulation 51 (a) and (b), and 26 dB for measurement 51 (c) and (d). It is true that the appeared FWM products are comparable with the noise at first look, but one should keep in mind, that:

1. equal channel spacing leads to FWM products creation at exactly same frequencies as the useful channels, which is the most harmful option for the lack of any ability to filter them out;
2. as it was proven above in this work, the highest power value is achieved by those FWM products, which frequencies are situated inside the channels or in a close proximity to them;

3. optical DWDM systems with more numerous channels, for example systems with 80 channels, will end up with both larger number of FWM products and also higher power values of FWM.

From these facts one may conclude that unequal channel spacing enables filtering majority of FWM products thus not allowing to damage a channel by inserting itself inside it; the less number of channels of a DWDM system is used, the less powerful FWM products will be raised.

Simulated and measured results differ in OSNR value, which may be explained by not taking into account the same number of used connectors at the measurement. Different channel power values were achieved in the measurements and simulations due to the fact that certain factors are not taken into consideration even though not disqualifying credibility of the result under inextricably ideal simulation conditions. The real output signal usually exhibited a lower power value than the simulated one.

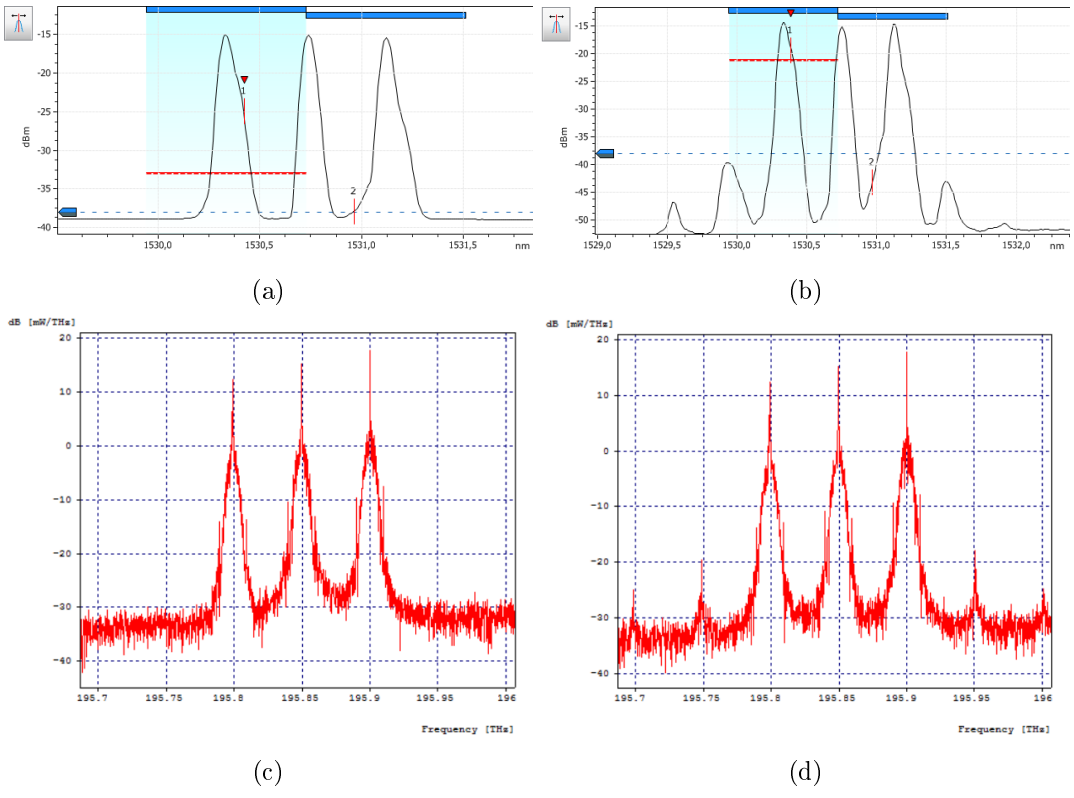

Figure 51: Measured and simulated values of output signal power

9 Conclusion

Four wave mixing produces new optical frequency components in DWDM systems, where its channels are closely spaced to one another. Not following the rules in order to mute or minimalize new FWM products creation can result in interchannel crosstalks in DWDM. All the conditions that raise the FWM phenomenon were practically proven in this work by simulations and practical experiments, which helped create a well-defined procedure to intelligible analysis and network planning, whereupon the best solution to avoid it can be found. These rules are the following:

- Using the correct channel spacing.
  Too small channel spacing can facilitate FWM products generation. The most appropriate channel spacing according to ITU-T is 100 GHz, 50 GHz, 25 GHz and 12.5 GHz. The wider the channel spacing is, the farther new destroying frequencies will be generated from the channels, and the easier it will be to filter them out;

- Spacing channels unequally.
  It is a more harmful option, when FWM generates new products at frequencies that coincide with channels that carry a useful signal. In this case FWM noise interferes the most for the lack of any ability to filter it out;

- Setting lower power of laser sources.
  The highest power value of FWM is achieved by those products, which frequencies are situated inside the channels or in a close proximity to them. The lower the power of laser sources is set, the more FWM energy is forwarded to lateral FWM products, so the less the useful channels are damaged by FWM;

- Using non-zero dispersion shifted fibers.
  On one hand, zero chromatic dispersion is the primary provocative factor of FWM. On the other hand, DWDM frequencies require phase synchronization in order to avoid pulse spreading in time so that the signal could be transmitted over long distances. This is one reason why it is necessary to use NZDSF optical fibers, which dispersion is close to zero. One should also not forget, that high dispersion value damage the BER of any signal, so dispersion of 5 ps/nm/km is considered to be the threshold value;

- Prevent using of high power of amplifiers.
  Instead of one amplifier or a cascade of amplifiers one by one, the first amplifier should be inserted before the optical fiber and the other one behind the fiber. Such a model

"dual-phase amplifier" does not cause FWM effect, and power at the output of the cascade is not reduced.

Not following any of these rules leads to the FWM creation. Any combination of conditions that give rise to FWM products will only have a more negative effect on the output signal. One should not neglect to follow these rules especially when working with optical DWDM systems having more numerous channels, for example systems with 80 channels, for in this case the receiving side will have to cope with both larger number of FWM products and also higher power values of FWM.

The greatest benefit of this work is systematization in the four wave mixing area and introduction of the rules to follow when arranging a DWDM based network. The goals set in the work assignment are completely met. The future work can be targeted at further parameters related to FWM generation, such as the use of different modulation formats.

A Rec. ITU-T G.694.1 (02/2012)

Table 11: Example nominal central frequencies of the DWDM grid [23]

Nominal central frequencies (THz) for spacing of:				Approximate nominal central wavelengths (nm) (Note)
12.5 GHz	25 GHz	50 GHz	100 GHz and above	
*	*	*	*	*
*	*	*	*	*
*	*	*	*	*
195.9375	—	—	—	1530.0413
195.9250	195.925	—	—	1530.1389
195.9125	—	—	—	1530.2365
195.9000	195.900	195.90	195.9	1530.3341
195.8875	—	—	—	1530.4318
195.8750	195.875	—	—	1530.5295
195.8625	—	—	—	1530.6271
195.8500	195.850	195.85	—	1530.7248
195.8375	—	—	—	1530.8225
195.8250	195.825	—	—	1530.9203
195.8125	—	—	—	1531.0180
195.8000	195.800	195.80	195.8	1531.1157
195.7875	—	—	—	1531.2135
195.7750	195.775	—	—	1531.3112
195.7625	—	—	—	1531.4090

Continued on next page

Table 11 – continued from previous page

Nominal central frequencies (THz) for spacing of:				Approximate nominal central wavelengths (nm) (Note)
12.5 GHz	25 GHz	50 GHz	100 GHz and above	
195.7500	195.750	195.75	—	1531.5068
195.7375	—	—	—	1531.6046
195.7250	195.725	—	—	1531.7024
195.7125	—	—	—	1531.8003
195.7000	195.700	195.70	195.7	1531.8981
195.6875	—	—	—	1531.9960
195.6750	195.675	—	—	1532.0938
195.6625	—	—	—	1532.1917
*	*	*	*	*
*	*	*	*	*
*	*	*	*	*
193.2375	—	—	—	1551.4197
193.2250	193.225	—	—	1551.5200
193.2125	—	—	—	1551.6204
193.2000	193.200	193.20	193.2	1551.7208
193.1875	—	—	—	1551.8212
193.1750	193.175	—	—	1551.9216
193.1625	—	—	—	1552.0220
193.1500	193.150	193.15	—	1552.1225
193.1375	—	—	—	1552.2229
193.1250	193.125	—	—	1552.3234
193.1125	—	—	—	1552.4239
193.1000	193.100	193.10	193.1	1552.5244

Continued on next page

Table 11 – continued from previous page

Nominal central frequencies (THz) for spacing of:				Approximate nominal central wavelengths (nm) (Note)
12.5 GHz	25 GHz	50 GHz	100 GHz and above	
193.0875	—	—	—	1552.6249
193.0750	193.075	—	—	1552.7254
193.0625	—	—	—	1552.8259
193.0500	193.050	193.05	—	1552.9265
193.0375	—	—	—	1553.0270
193.0250	193.025	—	—	1553.1276
193.0125	—	—	—	1553.2282
193.0000	193.000	193.00	193.0	1553.3288
192.9875	—	—	—	1553.4294
192.9750	192.975	—	—	1553.5300
192.9625	—	—	—	1553.6307
*	*	*	*	*
*	*	*	*	*
*	*	*	*	*
184.7750	184.775	—	—	1622.4731
184.7625	—	—	—	1622.5828
184.7500	184.750	184.75	—	1622.6926
184.7375	—	—	—	1622.8024
184.7250	184.725	—	—	1622.9122
184.7125	—	—	—	1623.0220
184.7000	184.700	184.70	184.7	1623.1319
184.6875	—	—	—	1623.2417
184.6750	184.675	—	—	1623.3516

Continued on next page

Table 11 – continued from previous page

Nominal central frequencies (THz) for spacing of:				Approximate nominal central wavelengths (nm) (Note)
12.5 GHz	25 GHz	50 GHz	100 GHz and above	
184.6625	—	—	—	1623.4615
184.6500	184.650	184.65	—	1623.5714
184.6375	—	—	—	1623.6813
184.6250	184.625	—	—	1623.7912
184.6125	—	—	—	1623.9012
184.6000	184.600	184.60	184.6	1624.0111
184.5875	—	—	—	1624.1211
184.5750	184.575	—	—	1624.2311
184.5625	—	—	—	1624.3411
184.5500	184.550	184.55	—	1624.4511
184.5375	—	—	—	1624.5612
184.5250	184.525	—	—	1624.6712
184.5125	—	—	—	1624.7813
184.5000	184.500	184.50	184.5	1624.8914
*	*	*	*	*
*	*	*	*	*
*	*	*	*	*

B Optical path arrangement used in section 6.4

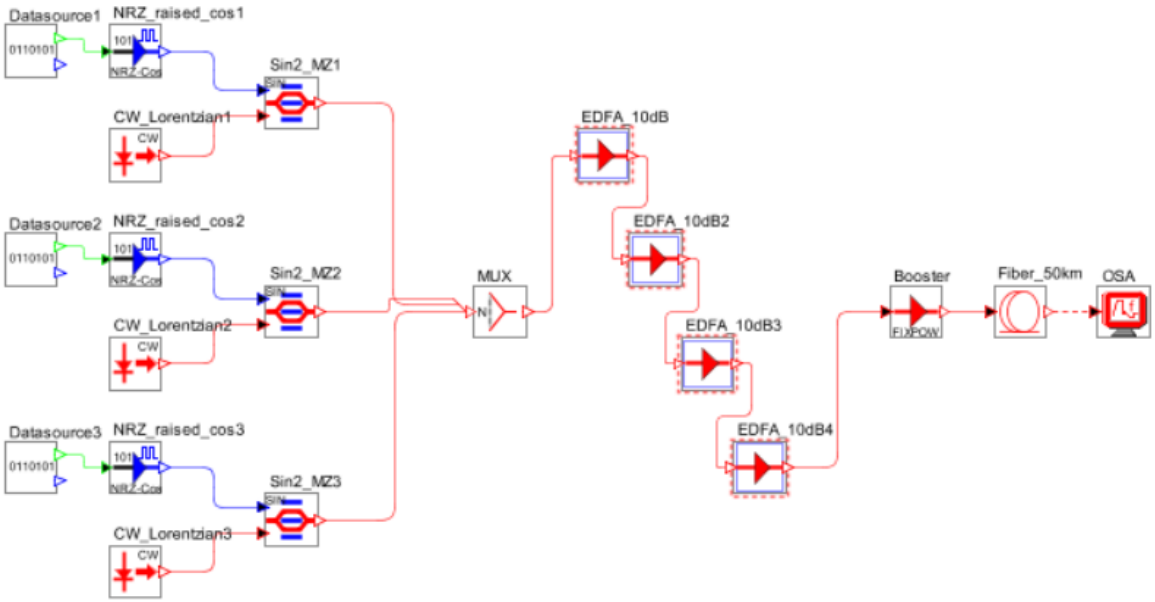

Figure 52: Complete optical path arrangement for raising the non-degenerate FWM phenomenon using three laser sources

C Output signal depending on spectral position of the tunable laser used in sections 8.1, 8.2 and 8.3

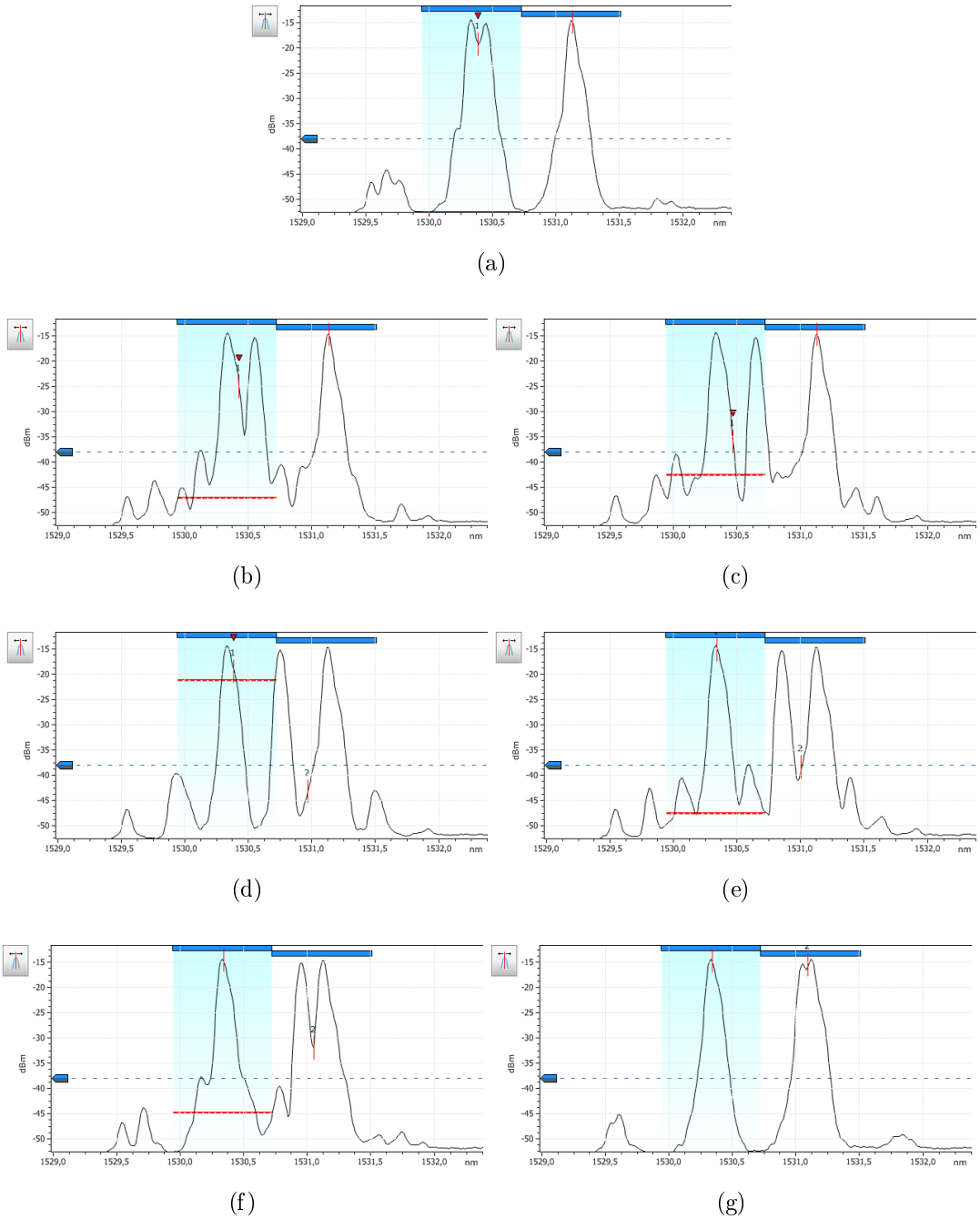

(a)

(b)

(c)

(d)

(e)

(f)

(g)

Figure 53: Output signal depending on spectral position of the tunable laser λ_2: a) $\lambda_2 = \lambda_1 + 0.1$ nm, b) $\lambda_2 = \lambda_1 + 0.2$ nm, c) $\lambda_2 = \lambda_1 + 0.3$ nm, d) $\lambda_2 = \lambda_1 + 0.4$ nm, e) $\lambda_2 = \lambda_1 + 0.5$ nm, f) $\lambda_2 = \lambda_1 + 0.6$ nm, g) $\lambda_2 = \lambda_1 + 0.7$ nm

References

[1] ERBIUM DOPED FIBER EDUCATION SYSTEMS. https://www.idil-fibres-optiques.com/wp-content/themes/idil/pdf/erbium-doped-fiber-IDIL-Fibres-Optiques.pdf. Accessed: 2018-05-14.

[2] Fiber-Optics.info. http://www.fiber-optics.info/. Accessed: 2018-05-08.

[3] FLS-2600B Tunable Laser Source, User Guide. https://www.profiber.eu/files/produkty/meracia%20technika_opticke_komunikacie/laboratoria_a_vyroba_vlaknovej_optiky/Tunable_Laser_Source_FLS_2600B/User_Guide_FLS_2600B_english_1061853.pdf. Accessed: 2018-05-14.

[4] FTB-500 Platform. https://www.exfo.com/umbraco/surface/file/download/?ni=10906&cn=en-US&pi=5415. Accessed: 2018-05-14.

[5] IQS/FLS-2600B TUNABLE LASER SOURCE, Spec Sheet. https://www.profiber.eu/files/produkty/meracia%20technika_opticke_komunikacie/laboratoria_a_vyroba_vlaknovej_optiky/Tunable_Laser_Source_FLS_2600B/EXFO_spec-sheet_IQS-FLS-2600B-v8_en.pdf. Accessed: 2018-05-14.

[6] QuickSpecs HP V1910 Switch Series. https://h20195.www2.hpe.com/v2/getpdf.aspx/c03824531.pdf?ver=4. Accessed: 2018-05-14.

[7] S7FC/S9FC Series Single-Channel Semiconductor and Booster Optical Amplifiers, Operating Manual. https://www.thorlabs.com/drawings/70d3d05b04c90f54-B2E3FBE2-9576-4CDF-02A8551B85F88301/S7FC1013S-Manual.pdf. Accessed: 2018-05-14.

[8] Rajdi Agalliu and Michal Lucki. System performance and limits of optical modulation formats in dense wavelength division multiplexing systems. *Elektronika ir Elektrotechnika*, 22(2):123–129, 2016.

[9] MH Al-Mansoori, WS Al-Ghaithi, and FN Hasoon. 55 db high gain l-band edfa utilizing single pump source. *World Academy of Science, Engineering and Technology, International Journal of Computer, Electrical, Automation, Control and Information Engineering*, 8(7):1201–1203, 2014.

[10] Rinu Ann Baby, Neenu Therese Antony, and Lin Ann Jose. Amplified dwdm communication network: An approach to analyze the characteristic performance. In *Wireless and*

Optical Communications Networks (WOCN), 2015 Twelfth International Conference on, pages 1–5. IEEE, 2015.

[11] Richa Bhatia, Ajay K Sharma, and Jyoti Saxena. Optimized alternate polarization and four wave mixing in 60-gb/s dwdm transmission system. In *Engineering and Computational Sciences (RAECS), 2014 Recent Advances in*, pages 1–4. IEEE, 2014.

[12] Vjačeslavs Bobrovs and G Ivanovs. Comparison of different modulation formats and their compatibility with wdm transmission system. *Latvian journal of Physics and technical sciences*, 45(2):3–16, 2008.

[13] Antonella Bogoni and Luca Poti. Effective channel allocation to reduce inband fwm crosstalk in dwdm transmission systems. *IEEE Journal of selected topics in Quantum Electronics*, 10(2):387–392, 2004.

[14] Leoš Boháč. Optické sítě. *Data.cedupoint.cz*, 2013. Online, available from: http://docplayer.cz/12633121-Opticke-site-leos-bohac.html.

[15] Farag Z El-Halafawy, Moustafa H Aly, and Maha A Abd El-Bary. Four-wave mixing crosstalk in dwdm optical fiber systems. In *Radio Science Conference, 2006. NRSC 2006. Proceedings of the Twenty Third National*, pages 1–6. IEEE, 2006.

[16] Bassem Fahs, Asif Jahangir Chowdhury, and Mona Mostafa Hella. A 12-m 2.5-gb/s lighting compatible integrated receiver for ook visible light communication links. *Journal of Lightwave Technology*, 34(16):3768–3775, 2016.

[17] Wolfgang Freude, René Schmogrow, Bernd Nebendahl, Marcus Winter, Arne Josten, David Hillerkuss, Swen Koenig, Joachim Meyer, Michael Dreschmann, Michael Huebner, et al. Quality metrics for optical signals: eye diagram, q-factor, osnr, evm and ber. In *Transparent Optical Networks (ICTON), 2012 14th International Conference on*, pages 1–4. IEEE, 2012.

[18] McGraw Hill Gerd Keiser. *Optical fiber communications, 3rd ed.* 2000.

[19] Hafiz Abd El Latif Ahmed Habib and DR RAZALI BIN NGAH. *Four wave mixing nonlinearity effect in wave length division multiplexing Radio over Fiber system.* PhD thesis, Citeseer, 2007.

[20] Anes Hodzic. Investigations of high bit rate optical transmission systems employing a channel data rate of 40 gb/s. *Dr Ingenieur thesis, Technische Universität Berlin*, 2004.

[21] Rec ITU-T. G. 655. *Characteristics of a non-zero dispersion-shifted single-mode optical fibre and cable*, November 2009. International Telecommunication Union.

[22] Rec ITU-T. G. 653. *Characteristics of a dispersion-shifted, single-mode optical fibre and cable*, July 2010. International Telecommunication Union.

[23] Rec ITU-T. G. 694.1. *Spectral grids for WDM applications: DWDM frequency grid*, February 2012. International Telecommunication Union.

[24] Rec ITU-T. G. 652. *Characteristics of a single-mode optical fibre and cable*, November 2016. International Telecommunication Union.

[25] John A Jay. An overview of macrobending and microbending of optical fibers. *White paper of Corning*, pages 1–21, 2010.

[26] Stanislav Kraus. Měření na dwdm systému. *Praha: České vysoké učení technické, Fakulta elektrotechnická,[cit. 10. 1. 2014]. Dostupné z:< http://data. cedupoint. cz/oppa_ e-learning/2_ KME/075. pdf.*

[27] Rupendra Maharjan, Ingrida Lavrinovica, Andis Supe, and Jurgis Porins. Minimization of fwm effect in nonlinear optical fiber using variable channel spacing technique. In *Advances in Wireless and Optical Communications (RTUWO), 2016*, pages 1–4. IEEE, 2016.

[28] Habib Ullah Manzoor, Abaid Ullah Salfi, Tayyab Mehmood, and Tareq Manzoor. Reduction of four wave mixing by employing circular polarizers in dwdm optical networks. In *Applied Sciences and Technology (IBCAST), 2015 12th International Bhurban Conference on*, pages 637–640. IEEE, 2015.

[29] Hassan M Oubei, José R Durán, Bilal Janjua, Huai-Yung Wang, Cheng-Ting Tsai, Yu-Cheih Chi, Tien Khee Ng, Hao-Chung Kuo, Hau He, Mohamed-Slim Alouini, et al. Wireless optical transmission of 450 nm, 3.2 gbit/s 16-qam-ofdm signals over 6.6 m underwater channel. In *Lasers and Electro-Optics (CLEO), 2016 Conference on*, pages 1–2. IEEE, 2016.

[30] Brian Pamukti and Doan Perdana. Non-linear effects of high rate soliton transmission on dwdm optical fiber communication system. In *Information Technology, Information Systems and Electrical Engineering (ICITISEE), International Conference on*, pages 26–30. IEEE, 2016.

[31] Bijayananda Patnaik and PK Sahu. Optimization of four wave mixing effect in radio-over-fiber for a 32-channel 40-gbps dwdm system. In *Electronic System Design (ISED), 2010 International Symposium on*. IEEE, 2010.

[32] AV Ramprasad, M Meenakshi, G Geetha, et al. Suppression of four wave mixing crosstalk components in dwdm optical systems. In *Wireless and Optical Communications Networks, 2006 IFIP International Conference on*, pages 5–pp. IEEE, 2006.

[33] Kasper Meldgaard Røge, Pengyu Guan, Hans Christian Hansen Mulvad, Niels-Kristian Kjøller, Michael Galili, Toshio Morioka, and Leif Katsuo Oxenløwe. Flexible dwdm grid manipulation using four wave mixing-based time lenses. In *Photonics Conference (IPC), 2014 IEEE*, pages 310–311. IEEE, 2014.

[34] A Selvamani and T Sabapathi. Suppression of four wave mixing by optical phase conjugation in dwdm fiber optic link. In *Recent Advancements in Electrical, Electronics and Control Engineering (ICONRAEeCE), 2011 International Conference on*, pages 95–99. IEEE, 2011.

[35] Neeraj Sharma, Robin Vij, and Neha Badhan. Enhanced spectral efficiency for intensity modulated dwdm systems. In *Communications (NCC), 2015 Twenty First National Conference on*, pages 1–6. IEEE, 2015.

[36] Federico Tosco. *Fiber optic communications handbook*. TAB Professional and Reference Books, 1990.

[37] Vardges Vardanyan. Single-fiber optical transmission system with dwdm channels effect of four-wave mixing products. In *Actual Problems of Electronics Instrument Engineering (APEIE), 2016 13th International Scientific-Technical Conference on*, volume 2, pages 23–25. IEEE, 2016.

[38] Robin Vij and Neeraj Sharma. 1b/s/hz spectrally efficient transmission for an 8 channel rz modulated dwdm systems. In *Control, Instrumentation, Energy and Communication (CIEC), 2014 International Conference on*, pages 513–518. IEEE, 2014.